AD-A074 831 SYRACUSE UNIV NY DEPT OF ELECTRICAL AND COMPUTER EN--ETC F/G 20/14
ELECTROMAGNETIC TRANSMISSION THROUGH AN ANNULAR APERTURE IN AN --ETC(U)
SEP 79 C CHA, R F HARRINGTON N00014-76-C-0225
UNCLASSIFIED TR-79-11 NL

| OF |
AD
A074831

END
DATE
FILMED
11-79
DDC

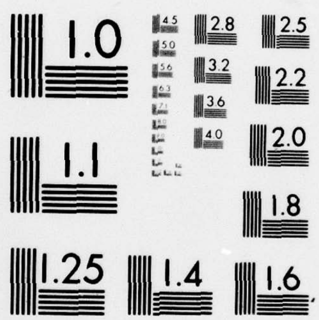

MICROCOPY RESOLUTION TEST CHART
NATIONAL BUREAU OF STANDARDS-1963-A

AD A074831

UNCLASSIFIED

SECURITY CLASSIFICATION OF THIS PAGE (When Data Entered)

REPORT DOCUMENTATION PAGE		READ INSTRUCTIONS BEFORE COMPLETING FORM
1. REPORT NUMBER (14) TR-79-11	2. GOVT ACCESSION NO.	3. RECIPIENT'S CATALOG NUMBER (9)
4. TITLE (and Subtitle) (6) ELECTROMAGNETIC TRANSMISSION THROUGH AN ANNULAR APERTURE IN AN INFINITE CONDUCTING SCREEN		5. TYPE OF REPORT & PERIOD COVERED Technical Report No. 11
		6. PERFORMING ORG. REPORT NUMBER
7. AUTHOR(s) (10) Chung-Chi Cha, Roger F. Harrington		8. CONTRACT OR GRANT NUMBER(s) (15) N00014-76-C-0225
9. PERFORMING ORGANIZATION NAME AND ADDRESS Dept. of Electrical and Computer Engineering, Syracuse University, Syracuse, New York 13210		10. PROGRAM ELEMENT, PROJECT, TASK AREA & WORK UNIT NUMBERS
11. CONTROLLING OFFICE NAME AND ADDRESS Department of the Navy, Office of Naval Research, Arlington, Virginia 22217		12. REPORT DATE (11) September 1979
		13. NUMBER OF PAGES 90
14. MONITORING AGENCY NAME & ADDRESS (if different from Controlling Office) (12) 93		15. SECURITY CLASS. (of this report) UNCLASSIFIED
		15a. DECLASSIFICATION/DOWNGRADING SCHEDULE

16. DISTRIBUTION STATEMENT (of this Report)

Approved for public release; distribution unlimited

17. DISTRIBUTION STATEMENT (of the abstract entered in Block 20, if different from Report)

18. SUPPLEMENTARY NOTES

19. KEY WORDS (Continue on reverse side if necessary and identify by block number)

Annular apertures	Electromagnetic fields
Apertures in planes	Equivalence principle
Circular apertures	Generalized admittances
Computer programs	Method of moments

20. ABSTRACT (Continue on reverse side if necessary and identify by block number)

Electromagnetic transmission through an annular aperture in an infinite conducting screen of zero thickness is investigated. The circular aperture is included as a special case. The fields on both sides of the screen are obtained from the free space Green's function by means of the equivalence principle and image theory. An integral equation for the equivalent magnetic current in the aperture is established by enforcing the continuity of the tangential components of both the electric and the magnetic field. This integral → next page

DD FORM 1 JAN 73 1473 EDITION OF 1 NOV 65 IS OBSOLETE

S/N 0102-014-6601

UNCLASSIFIED

SECURITY CLASSIFICATION OF THIS PAGE (When Data Entered)

406 737

JB

20. ABSTRACT (cont.)

equation is solved by the method of moments to obtain the magnetic current, from which other transmission characteristics are obtained.

NOTATION

$\underline{A}$	a vector in three dimensional space.
$\underline{\tilde{A}}$	an operator which, when operating on an element in its domain, gives a vector.
$\bar{A}_{N\times 1} = [A_q]_{N\times 1}$	a column matrix with dimension $N\times 1$ and A_q as its qth element (dimension is sometimes omitted when understood).
$\overset{\approx}{A}_{M\times N} = [A_{pq}]_{M\times N}$	a matrix operator with dimension $M\times N$ and A_{pq} as its element in the pth row and the qth column (dimension is sometimes omitted when understood).

Superscript * denotes the complex conjugate of the quantity.

Superscript T denotes the transpose of the matrix.

CONTENTS

I. INTRODUCTION

The problem of penetration of electromagnetic waves through an annular aperture in an infinite conducting screen of zero thickness is examined in the frequency domain. The formulation includes the circular aperture as a special case. The generalized network formulation for aperture problems by Harrington and Mautz [1] is used. The method of solution is, in general, a specialization of that for bodies of revolution by the above authors [2].

In the formulation, the equivalence principle [3] is used to establish an integral equation for the unknown magnetic current in the aperture. The method of moments [4] is used to solve this integral equation with expansion functions chosen to be harmonic in ϕ (azimuth angle) and subsectional in ρ (radial variable in the aperture). Because of the circular symmetry, Fourier modes are decoupled to one another and only matrices of considerably smaller sizes need to be dealt with one at a time.

Numerical results for the magnetic currents, radiation patterns, and transmission coefficients are given for some sample cases for both normal incidence and oblique incidence.

The assumption of a center conductor in the aperture in the present problem is difficult to realize in practice. However, further investigations of problems, such as wires and coaxial lines opening into a half space, may utilize some of the computer programs written. Also, results for complementary problems, such as scattering by conducting washers, can be obtained from the solution.

II. PROBLEM FORMULATION

The problem configuration is given in Fig. 1, which shows an annular aperture in a perfectly conducting screen with R_{in} and R_{out} as the inner and outer radius of the aperture, respectively. The conducting screen is infinite in the x and y directions and has zero thickness. Impressed sources $\underline{J}^i$ and $\underline{M}^i$, which produce $\underline{E}^{io}$ and $\underline{H}^{io}$ in the absence of the screen, exist in the region to the left of the screen (region a, $Z > 0$). The region to the right of the screen (region b, $Z < 0$) is source free. The unit normal $\underline{\hat{n}}$ is defined on the x-y plane as pointing away from region a.

The equivalence principle is utilized to separate the two regions as described in [1]. The aperture is covered by a perfect electric conductor and the equivalent magnetic currents are used to produce the required tangential electric field where the aperture originally existed. The equivalent situations for regions a and b are shown in Fig. 2(a) and (b).

For region a, an equivalent magnetic current with surface density $\underline{M} = \underline{\hat{n}} \times \underline{E}$ ($\underline{E}$ denotes total electric field), which is nonzero only over the aperture, is placed just to the left of the plane. This magnetic current, together with $\underline{J}^i$ and $\underline{M}^i$, radiates in the presence of the complete conducting screen covering the entire x-y plane to produce the total field in region a.

For region b, an equivalent magnetic current with surface current density-$\underline{M}$ is placed just to the right of the plane to radiate, in the presence of the complete conducting screen, the total field in

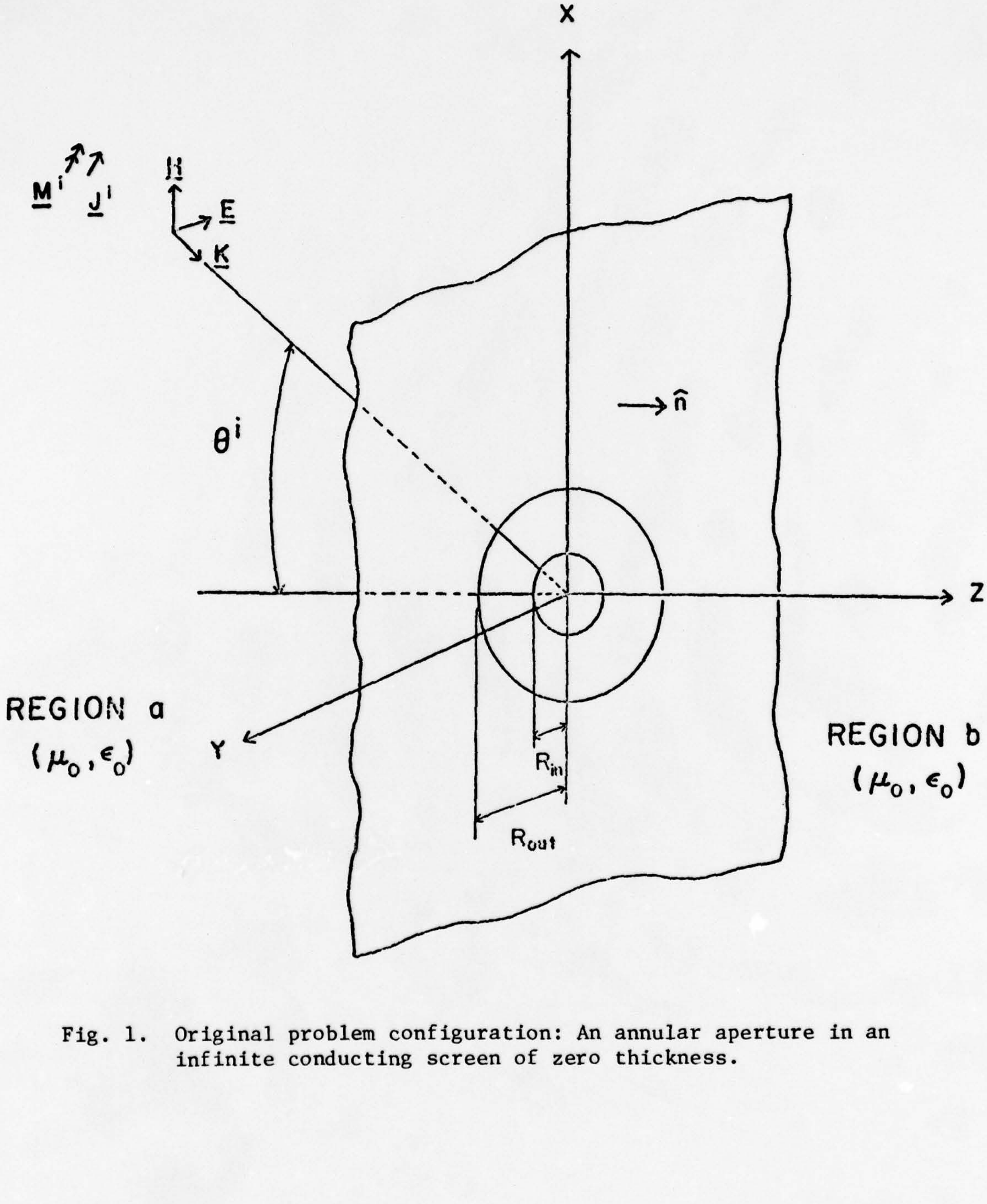

Fig. 1. Original problem configuration: An annular aperture in an infinite conducting screen of zero thickness.

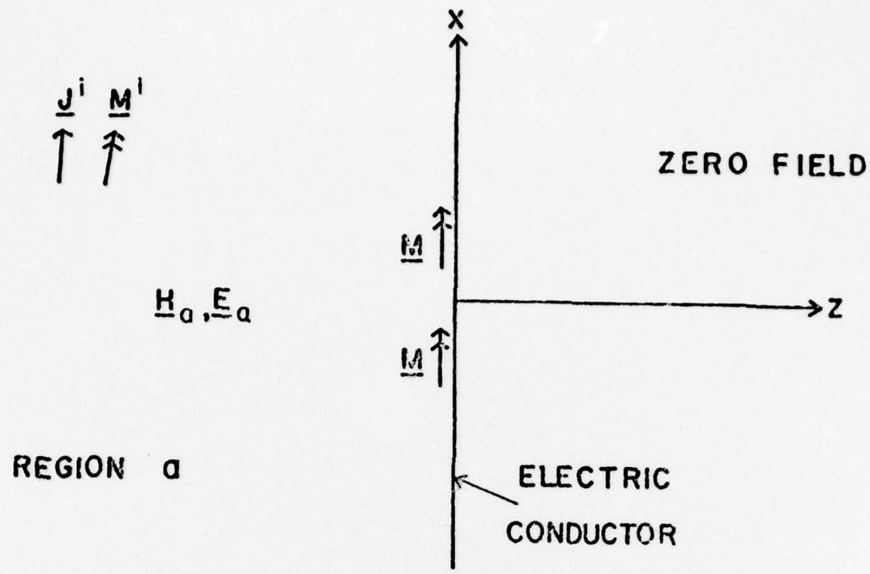

Fig. 2(a). Equivalence for region a.

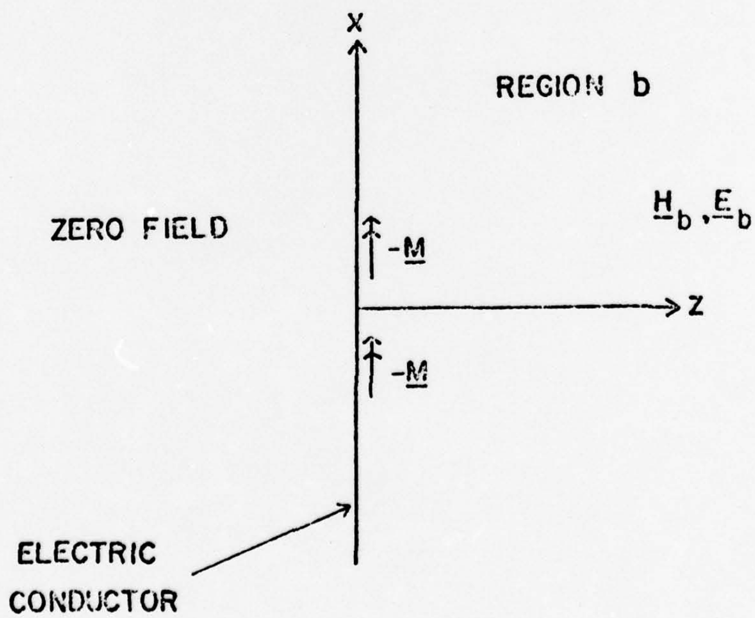

Fig. 2(b). Equivalence for region b.

region b. The use of $\underline{M}$ in region a and $-\underline{M}$ in region b assures the continuity of the tangential component of electric field across the aperture.

The magnetic field in region a, denoted $\underline{H}^a$, is the sum of that due to the impressed source, denoted $\underline{H}^i$, plus that due to the equivalent source $\underline{M}$, denoted $\underline{\tilde{H}}^a(\underline{M})$. Note that $\underline{H}^i$ is produced by $\underline{J}^i$ and $\underline{M}^i$ in the presence of the conducting plane and $\underline{\tilde{H}}^a$, operating on $\underline{M}$, gives the magnetic field in region a due to $\underline{M}$ in the presence of the conducting plane. Hence, we now have in region a,

$$\underline{H}^a = \underline{H}^i + \underline{\tilde{H}}^a(\underline{M}) \tag{1}$$

The magnetic field in region b, denoted $\underline{H}^b$, is that due to the magnetic current $-\underline{M}$, denoted $\underline{\tilde{H}}^b(-\underline{M})$. Hence, in region b, we have

$$\underline{H}^b = -\,\underline{\tilde{H}}^b(\underline{M}) \tag{2}$$

where the minus sign was factored out due to the linearity of the operator. Again note that $-\tilde{H}^b(\underline{M})$ gives the magnetic field produced by $-\underline{M}$ in the presence of the conducting plane in region b.

The boundary condition remaining to be satisfied is the continuity of the tangential magnetic field across the aperture. This gives, from (1) and (2),

$$-\underline{\hat{n}} \times \underline{\hat{n}} \times [\underline{\tilde{H}}^a(\underline{M}) + \underline{\tilde{H}}^b(\underline{M})] = \underline{\hat{n}} \times \underline{\hat{n}} \times \underline{H}^i \tag{3}$$

in the aperture region.

From image theory, we know that

$$\underline{\hat{n}} \times \underline{H}^{i} = \underline{\hat{n}} \times 2\ \underline{H}^{io} \tag{4}$$

in the aperture and also that $\underline{\tilde{H}}^{a} = \underline{\tilde{H}}^{b} = 2\ \underline{\tilde{H}}$ where $\underline{\tilde{H}}$ is defined by

$$\underline{\tilde{H}}(\underline{M}) = \frac{1}{4\pi} \Big\{ -\, j\omega\varepsilon_o \iint_{\text{aperture}} \frac{\underline{M}(\underline{r}')e^{-jk|\underline{r}-\underline{r}'|}}{|\underline{r}-\underline{r}'|}\, da' + \frac{1}{j\omega\mu_o} \nabla \iint_{\text{aperture}} \frac{[\nabla_t' \cdot \underline{M}(\underline{r}')]\ e^{-jk|\underline{r}-\underline{r}'|}}{|\underline{r}-\underline{r}'|}\, da' \Big\} \tag{5}$$

Here k is the wave number, ε_o and μ_o are free space permittivity and permeability, respectively, and the surface divergence operator is

$$\nabla_t' \cdot \underline{M}(\underline{r}') = \frac{\partial}{\partial x'}\ M_x(x',y') + \frac{\partial}{\partial y'}\ M_y(x',y') \tag{6}$$

where M_x and M_y denote the x and y components of $\underline{M}$.

From (4) and (5), (3) is now written as

$$-\ \underline{\hat{n}} \times \underline{\hat{n}} \times \underline{\tilde{H}}(\underline{M}) = \underline{\hat{n}} \times \underline{\hat{n}} \times \frac{1}{2}\ \underline{H}^{io} \tag{7}$$

in the aperture. Equation (7), together with the definition of $\underline{\tilde{H}}$ in (5), forms the basic equation for determining the equivalent magnetic current $\underline{M}$.

The method of moments is used to obtain an approximate solution $\underline{M}_o$ from (7). Let $\underline{M}_o$ be a linear combination of a finite set of vector "expansion" functions, $\{\underline{M}_q\}$, defined over the aperture region

$$\underline{M}_o = \sum_{q=1}^{N_o} V_q\ \underline{M}_q \tag{8}$$

A symmetric product of two vector functions over the aperture is defined as

$$<\underline{A},\underline{B}> = \iint_{\text{aperture}} \underline{A} \cdot \underline{B}\, da \qquad (9)$$

A finite set of vector "testing" functions $\{\underline{W}_p\}$ is also defined over the aperture region. We assume that the number of elements of $\{\underline{M}_q\}$ is N_o, the same as the number of elements of $\{\underline{W}_p\}$.

A matrix equation

$$[Y_{pq}]_{N_o \times N_o} \bar{V} = \bar{I} \qquad (10)$$

is then obtained by requiring that the symmetric product of each $\underline{W}_p$ with each side of (7), with $\underline{M}_o$ substituted for $\underline{M}$, be the same. In (10), $\bar{V}$ is a column matrix with dimension N_o whose elements are coefficients of the expansion of $\underline{M}_o$ defined in (8), that is,

$$\bar{V} = [V_q]_{N_o \times 1} \qquad (11)$$

The $\bar{I}$ is also a column matrix, called excitation matrix, of dimension N_o

$$\bar{I} = [I_p]_{N_o \times 1} \qquad (12)$$

where I_p is defined by

$$I_p = - <\underline{W}_p, \underline{\hat{n}} \times \underline{\hat{n}} \times \frac{1}{2} \underline{H}^{io}> \qquad (13)$$

The $[Y_{pq}]_{N_o \times N_o}$ is a square matrix, called admittance matrix, of dimension $N_o \times N_o$ whose elements are defined by

$$Y_{pq} = <\underline{W}_p, \underline{\hat{n}} \times \underline{\hat{n}} \times H(\underline{M}_q)> \qquad (14)$$

Furthermore, if the testing functions are all tangential to the x-y plane, i.e.

$$\underline{W}_p \cdot \underline{\hat{n}} = 0 \quad \text{for } p=1,2,\ldots,N_o \qquad (15)$$

then (13) and (14) can be reduced to

$$I_p = \frac{1}{2} \langle \underline{W}_p, \underline{H}^{io} \rangle \tag{16}$$

and

$$Y_{pq} = - \langle \underline{W}_p, \underline{\tilde{H}}(\underline{M}_q) \rangle \tag{17}$$

The problem now is to determine the column matrix $\bar{V}$ which, from (10), is given by

$$\bar{V} = [Y_{pq}]^{-1}\bar{I} \tag{18}$$

when the inverse of $[Y_{pq}]$, denoted $[Y_{pq}]^{-1}$, is assumed to exist.

III. PROBLEM SPECIALIZATION

In this Section the expansion and testing functions used in solving the problem, and also the type of incident fields under consideration, are specified.

(a) Expansion and Testing Functions

The expansion and testing functions are described in polar coordinates in the x-y plane. The domain $[R_{in}, R_{out}]$ is divided into M equal subintervals with a uniform length

$$\Delta = \frac{d}{M} \tag{19}$$

where

$$d = R_{out} - R_{in} \tag{20}$$

A set of nodes are defined at the boundaries of those subintervals

$$\rho_\ell = R_{in} + \ell\Delta \tag{21}$$

for $\ell = 0,1,2,\ldots,M$.

For expansion functions, we use

$$\underline{M}_q(\rho,\ \phi) = \hat{\underline{u}}_s\ f_{s\ell}(\rho)e^{jn\phi} \tag{22}$$

where

$$q(s,\ell,\ n) = (n+N)\ (2M-1) + \nu_s(M-1) + \ell \tag{23}$$

for $\quad s = \rho,\phi$

$\ell = 1,2,\ldots,L_s$

$n = -N,\ -(N-1),\ldots,(N-1),N$

and ν_s is defined as

$$\nu_s = \begin{cases} 0 & \text{if } s = \rho \\ 1 & \text{if } s = \phi \end{cases} \tag{24}$$

L_s is defined as

$$L_s = \begin{cases} M-1 & \text{if } s = \rho \\ M & \text{if } s = \phi \end{cases} \tag{25}$$

and $f_{s\ell}(\rho)$ is defined as

$$f_{\rho\ell}(\rho) = \frac{P_{\ell+\frac{1}{2}}(\rho)}{(\rho/d)} \tag{26}$$

$$f_{\phi\ell} = P_\ell(\rho) \tag{27}$$

where

$$P_\ell(\rho) = \begin{cases} 1 & \text{for } \rho_\ell - \Delta \leq \rho \leq \rho_\ell \\ 0 & \text{elsewhere} \end{cases} \tag{28}$$

$$P_{\ell+\frac{1}{2}}(\rho) = P_\ell(\rho - \frac{\Delta}{2}) \tag{29}$$

For testing functions, we use

$$\underline{W}_p(\rho,\phi) = \hat{\underline{u}}_\tau g_{\tau i}(\rho)e^{-jm\phi} \tag{30}$$

where

$$P(\tau,i,m) = (N+m)(2M-1) + \nu_\tau(M-1) + i \tag{31}$$

for $\tau = \rho,\phi$

$i = 1,2,\ldots,L_\tau$

$m = -N, -(N-1),\ldots,(N-1),N$

and $g_{\tau i}(\rho)$ is defined as

$$g_{\rho i}(\rho) = c_1 f_{\rho i}(\rho) \tag{32}$$

$$g_{\phi i}(\rho) = c_2\ \delta(\rho - (\rho_i - \frac{\Delta}{2})) \tag{33}$$

where $$c_1 = \frac{2}{\Delta\pi d} \tag{34}$$

$$c_2 = \frac{2}{\Delta\pi} \tag{35}$$

and δ is the Dirac delta function. The constants c_1 and c_2 are used to avoid possible unnecessary common factors of $\tilde{\tilde{Y}}$ and $\bar{I}$ in their final forms.

(b) Incident Fields $\underline{E}^{io}$ and $\underline{H}^{io}$

The incident fields considered here are plane waves, which are good approximations for fields radiated by sources distant from the aperture region. The propagation vector $\underline{k}$ is assumed to lie in the x-z plane, and the angle of incidence, θ^i, is defined as:

$$\theta^i = \cos^{-1}(\hat{\underline{u}}_k \cdot \hat{\underline{u}}_z) \qquad 0 \leq \theta^i \leq \frac{\pi}{2} \tag{36}$$

where

$$\hat{\underline{u}}_k = \underline{k}/|\underline{k}| \tag{37}$$

For each propagation vector $\underline{k}$, two unit vectors $\hat{\underline{u}}_\perp$ and $\hat{\underline{u}}_{/\!/}$ are defined:

$$\underline{\hat{u}}_{\perp} = - \underline{\hat{u}}_{y} \tag{38}$$

$$\underline{\hat{u}}_{/\!/} = \underline{\hat{u}}_{y} \times \underline{\hat{u}}_{k} \tag{39}$$

The incident plane waves considered are of the form

$$\underline{E}^{io} = E^{io}\, \underline{\hat{u}}_{e}\, e^{-j\underline{k} \cdot \underline{r}} \tag{40}$$

$$\underline{H}^{io} = \frac{\underline{\hat{u}}_{k}}{\eta_o} \times \underline{E}^{io} \tag{41}$$

where $\underline{\hat{u}}_e$ can be either $\underline{\hat{u}}_{\perp}$ or $\underline{\hat{u}}_{/\!/}$ and η_o denotes the free space impedance $\sqrt{\frac{\mu_o}{\varepsilon_o}}$.

When $\underline{\hat{u}}_e = \underline{\hat{u}}_{\perp}$, the incident waves above are said to be of vertical (denoted $E_{\perp}$) polarization and the polar components of the magnetic field in the aperture are:

$$H_{\rho}^{io} = \frac{E^{io}}{\eta_o} \cos \theta^i \cos \phi\; e^{-jk\rho \sin \theta^i \cos \phi} \tag{42}$$

$$H_{\phi}^{io} = - \frac{E^{io}}{\eta_o} \cos \theta^i \sin \phi\; e^{-jk\rho \sin \theta^i \cos \phi} \tag{43}$$

When $\underline{\hat{u}}_e = \underline{\hat{u}}_{/\!/}$, the incident waves in (40) and (41) are said to be of horizontal (denoted $E_{/\!/}$) polarization and,

$$H_{\rho}^{io} = \frac{E^{io}}{\eta_o} \sin \phi\; e^{-jk\rho \sin \theta^i \cos \phi} \tag{44}$$

$$H_{\phi}^{io} = \frac{E^{io}}{\eta_o} \cos \phi\; e^{-jk\rho \sin \theta^i \cos \phi} \tag{45}$$

in the aperture.

Notice that, although the two linear polarizations above are considered separately, the transmission of an elliptically polarized wave can be obtained from the results of these separate considerations. Appendix A gives a brief discussion of this.

IV. EVALUATION OF ADMITTANCE MATRIX AND EXCITATION MATRIX

(a) Admittance Matrix

In the preceding sections, the general formulation of the problem and the specification of expansion and testing functions have been given. In this section, approximations used in the computation of the admittance matrix $[Y_{pq}]$ are discussed. These approximations, together with some of the intermediate steps, are summarized and the final forms of the matrix elements are given.

(i) The surface divergence (6) can be written in its polar form as

$$\nabla_t \cdot \underline{A} = \frac{1}{\rho}\frac{\partial}{\partial\rho}(\rho A_\rho) + \frac{1}{\rho}\frac{\partial A_\phi}{\partial\phi} \tag{46}$$

where A_ρ, A_ϕ are polar components of $\underline{A}$. From (22) and (46), we have

$$\nabla'_t \cdot \underline{M}_q(\rho', \phi') = jn\, P_\ell(\rho')e^{jn\phi'}/\rho' \text{ for } s=\phi \tag{47}$$

Recall here that q is a function of s, ℓ and n and conversely, s, ℓ and n are each functions of q, as shown in (23).

To compute $\nabla'_t \cdot \underline{M}_q(\rho',\phi')$ for $s=\rho$, a finite difference approximation is used to spread out the impulse functions encountered:

$$\nabla'_t \cdot \underline{M}_q(\rho',\phi') = \frac{d}{\rho'}\frac{\partial}{\partial\rho'}[P_{\ell+\frac{1}{2}}(\rho')e^{jn\phi'}]$$

$$[P_\ell(\rho') - P_{\ell+1}(\rho')]e^{jn\phi'}/(\Delta\rho'/d)$$

$$\text{for } s=\rho \tag{48}$$

(ii) The admittance matrix elements are calculated according to (17) because the testing functions (30) are tangential to the x-y plane. Equation (17) is written here again with the subscripts of the elements written, explicitly, as functions.

$$Y_{pq} = - \langle \underline{W}_{p(s,\ell,n)}, \underline{\tilde{H}}(\underline{M}_{q(\tau,i,m)}) \rangle \tag{49}$$

where

$$p(s,\ell,n) = (n+N)(2M-1) + \nu_s(M-1) + \ell \tag{50}$$

$$q(\tau,i,m) = (m+N)(2M-1) + \nu_\tau(M-1) + i \tag{51}$$

and

$$\nu_s = \begin{cases} 0 & \text{if } s = \rho \\ 1 & \text{if } s = \phi \end{cases} \tag{52}$$

(iii) It can be shown that

$$\langle \underline{W}_{p(s,\ell,n)}, \underline{\tilde{H}}(\underline{M}_{q(\tau,i,m)}) \rangle = 0 \quad \text{for } m \neq n \tag{53}$$

and from this result, together with (49) to (52), equation (10) will look like

$$\begin{bmatrix} \tilde{\tilde{Y}}^{-N} & & & \\ & \tilde{\tilde{Y}}^{-(N-1)} & & \\ & & \ddots & \\ & & & \tilde{\tilde{Y}}^{N} \end{bmatrix} \begin{bmatrix} \bar{V}^{-N} \\ V^{-(N-1)} \\ \vdots \\ \bar{V}^{N} \end{bmatrix} = \begin{bmatrix} \bar{I}^{-N} \\ \bar{I}^{-(N-1)} \\ \vdots \\ \bar{I}^{N} \end{bmatrix} \tag{54}$$

there submatrices $\tilde{\tilde{Y}}^n$'s all have the same dimension (2M-1) × (2M-1) and can again be written in terms of their submatrices.

$$\tilde{\tilde{Y}}^n = \begin{bmatrix} [A^n_{i\ell}] & [B^n_{i\ell}] \\ [C^n_{i\ell}] & [D^n_{i\ell}] \end{bmatrix} \tag{55}$$

for $n = -N, -(N-1), \ldots, N$ and where

$$A^n_{i\ell} = - \langle \underline{W}_{p(\rho,i,n)}, \underline{\tilde{H}}(\underline{M}_{q(\rho,\ell,n)}) \rangle \tag{56}$$

for $i = 1,2,\ldots, M-1$

$\ell = 1,2,\ldots, M-1$

and

$$B^n_{i\ell} = - \langle \underline{W}_{p(\rho,i,n)}, \underline{\tilde{H}}(\underline{M}_{q(\phi,\ell,n)}) \rangle \tag{57}$$

for $i = 1,2,\ldots, M-1$

$\ell = 1,2,\ldots, M$

and

$$C^n_{i\ell} = - \langle \underline{W}_{p(\phi,i,n)}, \underline{\tilde{H}}(\underline{M}_{q(\rho,\ell,n)}) \rangle \tag{58}$$

for $i = 1,2,\ldots, M$

$\ell = 1,2,\ldots, M-1$

and

$$D^n_{i\ell} = - \langle \underline{W}_{p(\phi,i,n)}, \underline{\tilde{H}}(\underline{M}_{q(\phi,\ell,n)}) \rangle \tag{59}$$

for $i = 1,2,\ldots, M$

$\ell = 1,2,\ldots, M$

The column matrices $\bar{V}^n$'s and $\bar{I}^n$'s all have the same dimension (2M-1) and are defined as

$$\bar{V}^n = \begin{bmatrix} V^n_{\rho 1} \\ V^n_{\rho 2} \\ \vdots \\ V^n_{\rho(M-1)} \\ V^n_{\phi 1} \\ \vdots \\ V^n_{\phi M} \end{bmatrix} \tag{60}$$

$$\bar{I}^n = \begin{bmatrix} I^n_{\rho 1} \\ I^n_{\rho 2} \\ \vdots \\ I^n_{\rho(M-1)} \\ I^n_{\phi 1} \\ \vdots \\ I^n_{\phi M} \end{bmatrix} \tag{61}$$

where $V^n_{s\ell}$'s are coefficients of the expansion functions $\underline{M}_{q(s,\ell,n)}$'s and $I^n_{s\ell}$'s are defined by

$$I^n_{s\ell} = \frac{1}{2} \langle \underline{W}_{q(s,\ell,n)}, \underline{H}^{io} \rangle \tag{62}$$

for $s = \rho, \phi \quad \ell = 1,2,\ldots, L_s$.

From (54), we now have (2N+1) matrix equations of the form

$$\tilde{\tilde{Y}}^n \bar{V}^n = \bar{I}^n \qquad \text{for } n = -N, -(N-1), \ldots, N \tag{63}$$

with $\tilde{\tilde{Y}}^n$, $\bar{V}^n$ and $\bar{I}^n$ defined by (55)-(62).

(iv) Integrations in (5) and (9) are done in polar coordinates

$$\iint\limits_{aperture} da = \int_{R_{in}}^{R_{out}} \rho d\rho \int_{0}^{2n} d\phi \tag{64}$$

$$\iint\limits_{aperture} da' = \int_{R_{in}}^{R_{out}} \rho' d\rho' \int_{0}^{2n} d\phi' \tag{65}$$

(v) Inner products of unit vectors are summarized here:

$$\underline{\hat{u}}_{\rho} \cdot \underline{\hat{u}}_{\rho'} = \underline{\hat{u}}_{\phi} \cdot \underline{\hat{u}}_{\phi'} = \cos\,(\phi' - \phi) \tag{66}$$

$$\underline{\hat{u}}_{\phi} \cdot \underline{\hat{u}}_{\rho'} = -\,\underline{\hat{u}}_{\rho} \cdot \underline{\hat{u}}_{\phi'} = \sin\,(\phi' - \phi) \tag{67}$$

(vi) It can be shown that, for all admittance matrix elements, a single variable $(\phi'-\phi)$ in the angle direction is needed during the integration and thus a single variable ϕ, instead of $(\phi'-\phi)$, will be used from now on.

(vii) New variables are used for integrations according to

$$\rho = \Delta t \tag{68}$$

$$\rho' = \Delta t' \tag{69}$$

and

$$\phi = \frac{\pi}{2}\,(\theta + 1) \tag{70}$$

The last one is done for the convenience of numerical integration by Gaussian quadratures in the range of ϕ from 0 to π.

(viii) The pulse $P_{\ell+\frac{1}{2}}(\rho)$ is approximated by four impulses during the integration.

$$P_{\ell+\frac{1}{2}}(\rho) \approx \frac{1}{4} \sum_{m=1}^{4} \delta(\rho - \rho_{\ell m}) \tag{71}$$

where

$$\rho_{\ell m} = \rho_{\ell} + \frac{(m - 2.5)\Delta}{4} \tag{72}$$

(ix) The integration in θ (θ introduced in (70)) is approximated by the Gaussian-quadrature method

$$\int_{-1}^{1} d\theta\ f(\theta) \approx \sum_{m=1}^{N_g} w_m\ f(\theta_m) \tag{73}$$

where w_m's and θ_m's are the weight factors and abscissas of the N_gth order Gaussian-quadrature integration.

(x) The exponential

$$e^{-jkR}$$

where

$$R = \sqrt{\rho_{p\ell}^2 + \rho'^2 - 2\rho_{p\ell}\rho' \cos \phi_m} \tag{74}$$

with

$$\phi_m = \frac{\pi}{2} (\theta_m + 1)$$

is approximated by the first two terms of its Taylor series expansion about the value of R when ρ' assumes the mean value of its domain of integration, i.e.,

$$e^{-jkR} \approx e^{-jkR_o} [1 - jk(R - R_o)] \quad \text{for } \rho_a \leq \rho' \leq \rho_a + \Delta \tag{75}$$

where

$$R_o = \sqrt{\rho_{p\ell}^2 + \rho_c^2 - 2\rho_{p\ell}\ \rho_c \cos \phi_m} \tag{76}$$

$$\rho_c = \rho_a + \frac{\Delta}{2} \tag{77}$$

The validity of (75) is based on the condition

$$\frac{k\Delta}{2} << 1 \tag{78}$$

or, equivalently

$$\pi(\frac{\Delta}{\lambda}) << 1 \tag{79}$$

where λ is the wavelength of the wave.

The final forms of the admittance matrix elements are now given in terms of the submatrices $\tilde{\tilde{A}}^n$, $\tilde{\tilde{B}}^n$, $\tilde{\tilde{C}}^n$, $\tilde{\tilde{D}}^n$. Note that although approximations are involved as described in (i), (viii), (ix) and (x), equality signs are still used for simplicity.

$$A^n_{pq} = \frac{M}{\eta_o} \sum_{m=1}^{N_g} w_m \{\frac{j\kappa}{4} F_1(\theta_m)[\sum_{\ell=1}^{4} g_{\frac{1}{2}}(p,q,\ell,m)] - \frac{1}{j\kappa} F_3(\theta_m)[g(p,q,6,m) - g(p,q,5,m) + g(p,q+1,5,m) - g(p,q+1,6,m)]\} \tag{80}$$

$$B^n_{pq} = -\frac{1}{\eta_o} \sum_{m=1}^{N_g} w_m \{\frac{\kappa}{4} F_2(\theta_m)[\sum_{\ell=1}^{4} h(p,q,\ell,m)] + \frac{n}{\kappa} F_3(\theta_m)[g(p,q,6,m) - g(p,q,5,m)]\} \tag{81}$$

$$C^n_{pq} = \frac{M}{\eta_o} \sum_{m=1}^{N_g} w_m \{\kappa(x_p - \frac{1}{2}) F_2(\theta_m) g_{\frac{1}{2}}(p,q,5,m) - \frac{n}{\kappa} F_3(\theta_m)[g(p,q,5,m) - g(p,q+1,5,m)]\} \tag{82}$$

$$D^n_{pq} = \frac{1}{\eta_o} \sum_{m=1}^{N_g} w_m[j\kappa(x_p - \frac{1}{2}) F_1(\theta_m) h(p,q,5,m) + \frac{n^2}{j\kappa} F_3(\theta_m) g(p,q,5,m)] \tag{83}$$

where

$$\kappa = k\Delta \tag{84}$$

θ_m's and w_m's $(m = 1,2,\ldots\ldots,N_g)$ are the abscissas and weight factors of Gaussian-quadrature integration of order N_g as described in (ix), and

$$F_1(\theta_m) = \frac{1}{2}\,\{\cos[(n+1)\,\frac{\pi}{2}\,(\theta_m+1)] + \cos[(n-1)\,\frac{\pi}{2}\,(\theta_m+1)]\} \tag{85}$$

$$F_2(\theta_m) = \frac{1}{2}\,\{\cos[(n+1)\,\frac{\pi}{2}\,(\theta_m+1)] - \cos[(n-1)\,\frac{\pi}{2}\,(\theta_m+1)]\} \tag{86}$$

$$F_3(\theta_m) = \cos[n\,\frac{\pi}{2}\,(\theta_m+1)] \tag{87}$$

and

$$g(p,q,\ell,m) = \int_{x_{q-1}}^{x_q} \frac{e^{-j\kappa R_{p\ell m}}}{R_{p\ell m}}\,dt \tag{88}$$

$$g_{\frac{1}{2}}(p,q,\ell,m) = \int_{x_{q-1/2}}^{x_{q+1/2}} \frac{e^{-j\kappa R_{p\ell m}}}{R_{p\ell m}}\,dt \tag{89}$$

$$h(p,q,\ell,m) = \int_{x_{q-1}}^{x_q} \frac{t e^{-j\kappa R_{p\ell m}}}{R_{p\ell m}}\,dt \tag{90}$$

where

$$R_{p\ell m} = \sqrt{t^2 + x_{p\ell}^2 + 2t\,x_{p\ell}\,\sin\,[\frac{\pi}{2}\,\theta_m]} \tag{91}$$

$$x_q = x_o + q \qquad\qquad q = 0,\ \frac{1}{2},\ 1,\ \frac{3}{2},\ldots,M \tag{92}$$

$$x_{p\ell} = \frac{\rho_{p\ell}}{\Delta} = x_o + p + \frac{(\ell - 2.5)}{4} \qquad p = 1,2,\ldots,M-1;\quad \ell = 1,2,3,4 \tag{93}$$

$$x_o = R_{in}/\Delta \tag{94}$$

To evaluate g, $g_{\frac{1}{2}}$ and h, an approximation of $e^{-j\kappa R_{p\ell m}}$ as described in (x) is used with results as given below:

$$g(p,q,\ell,m) = e^{-j\kappa R_{p(q-1/2)\ell m}} [(1+j\ R_{p(q-1/2)\ell m})\ S_{pq\ell m} - j\kappa] \tag{95}$$

$$g_{1/2}(p,q,\ell,m) = g(p,q+1/2,\ell,m) \tag{96}$$

$$h(p,q,\ell,m) = e^{-j\kappa R_{p(q-1/2)\ell m}} \{(1+j\kappa R_{p(q-1/2)\ell m})[R_{pq\ell m} - R_{p(q-1)\ell m}$$

$$-x_{p\ell} \sin(\tfrac{\pi}{2}\theta_m)\ S_{pq\ell m}] - j\kappa(x_q - \tfrac{1}{2})\} \tag{97}$$

where

$$R_{pq\ell m} = R_{p\ell m}\Big|_{t=x_q}$$

$$S_{pq\ell m} = \ln\left[\frac{(t_{pq\ell m} + \frac{1}{2}) + \sqrt{(t_{pq\ell m} + \frac{1}{2})^2 + d^2_{p\ell m}}}{(t_{pq\ell m} - \frac{1}{2}) + \sqrt{(t_{pq\ell m} - \frac{1}{2})^2 + d^2_{p\ell m}}}\right]$$

and

$$t_{pq\ell m} = \left|x_q + x_{p\ell}\ \sin\left(\frac{\pi}{2}\ \theta_m\right) - \frac{1}{2}\right| \tag{100}$$

$$d^2_{p\ell m} = x^2_{p\ell}\ \cos^2\left(\frac{\pi}{2}\ \theta_m\right) \tag{101}$$

a different form of $S_{pq\ell m}$,

$$S_{pq\ell m} = \ln\left\{\frac{[(t_{pq\ell m} + \frac{1}{2}) + \sqrt{(t_{pq\ell m} + \frac{1}{2}) + d^2_{p\ell m}}\,][-(t_{pq\ell m} - \frac{1}{2}) + \sqrt{(t_{pq\ell m} - \frac{1}{2})^2 + d^2_{p\ell m}}\,]}{d^2_{p\ell m}}\right\} \tag{102}$$

is used for $t_{pq\ell m} < \frac{1}{2}$ to reduce numerical errors.

Notice, from the above formulas, the following symmetry exists:

$$\begin{bmatrix} [\bar{A}^n_{pq}] & [B^{-n}_{pq}] \\ [C^{-n}_{pq}] & [D^{-n}_{pq}] \end{bmatrix} = \begin{bmatrix} [A^n_{pq}] & -[B^n_{pq}] \\ -[C^n_{pq}] & [D^n_{pq}] \end{bmatrix} \tag{103}$$

(b) Excitation Matrix $[I_p]$

The excitation matrix is considered for the two polarizations described in Sec. III-(a).

(i) $E_{\perp}$-polarization

Substituting (30), (42) and (43) into (62), one obtains

$$I^n_{\rho q} = E^{io}\, i^{n\perp}_{\rho q} \tag{104}$$

$$I^n_{\phi q} = E^{io}\, i^{n\perp}_{\phi q} \tag{105}$$

where

$$i^{n\perp}_{\rho q} = i^{-n\perp}_{\rho q} = \frac{-1}{\eta_o}\, j^{-n+1} \cos\theta^i \int_{x_{q-1/2}}^{x_{q+1/2}} [J_{n+1}(\beta t) - J_{n-1}(\beta t)]dt \tag{106}$$

$$i^{n\perp}_{\phi q} = -\, i^{-n\perp}_{\phi q} = \frac{-1}{\eta_o}\, j^{-n}\, x_{q-1/2} \cos\theta^i [J_{n+1}(\beta x_{q-1/2}) + J_{n-1}(\beta x_{q-1/2})] \tag{107}$$

$$\beta = \kappa \sin\theta^i \tag{108}$$

The integral formula for Bessel functions,

$$J_n(x) = \frac{j^n}{2\pi} \int_0^{2\pi} e^{-jn\phi - jx\cos\phi}\, d\phi \tag{109}$$

is used.

It can be shown that, when $\frac{\kappa}{2} << 1$ (typically $\Delta \sim \frac{\lambda}{30}$), the following approximation for $i^{n\perp}_{\rho q}$ is of little error (typically 1%),

$$i^{n\perp}_{\rho q} = \frac{-1}{\eta_o}\, j^{-n+1} \cos\theta^i\, [J_{n+1}(\beta x_q) - J_{n-1}(\beta x_q)] \tag{110}$$

Now, a column matrix

$$\bar{v}^{n\perp} = \begin{bmatrix} \bar{v}^{n\perp}_{\rho} \\ \bar{v}^{n\perp}_{\phi} \end{bmatrix} = \begin{bmatrix} \begin{bmatrix} v^{n\perp}_{\rho 1} \\ \vdots \\ v^{n\perp}_{M-1} \end{bmatrix} \\ \begin{bmatrix} v^{n\perp}_{\rho 1} \\ \vdots \\ v^{n\perp}_{\phi M} \end{bmatrix} \end{bmatrix} \tag{111}$$

is introduced as the solution of the equation

$$\tilde{\bar{Y}}^{n} \, \bar{v}^{n\perp} = \bar{i}^{n\perp} \tag{112}$$

where

$$\bar{i}^{n\perp} = \begin{bmatrix} \bar{i}^{n\perp}_{\rho} \\ \bar{i}^{n\perp}_{\phi} \end{bmatrix} = \begin{bmatrix} \begin{bmatrix} i^{n\perp}_{\rho 1} \\ \vdots \\ i^{n\perp}_{\rho M-1} \end{bmatrix} \\ \begin{bmatrix} i^{n\perp}_{\phi 1} \\ \vdots \\ i^{n\perp}_{\phi M} \end{bmatrix} \end{bmatrix} \tag{113}$$

The magnetic current in this case can now be written as

$$\underline{M}_{o} = E^{io} \, (m^{\perp}_{\rho} \, \underline{\hat{u}}_{\rho} + m^{\perp}_{\phi} \, \underline{\hat{u}}_{\phi}) \tag{114}$$

where

$$m^{\perp}_{\rho} = T^{o}_{\rho} \, (\rho) + \sum_{n=1}^{N} T^{n}_{\rho c}(\rho) \cos n\phi \tag{115}$$

$$m^{\perp}_{\phi} = \sum_{n=1}^{N} T^{n}_{\phi s}(\rho) \sin n\phi \tag{116}$$

$$T_{\rho}^{o}(\rho) = \frac{d}{\rho} \sum_{q=1}^{M-1} v_{\rho q}^{o\perp} P_{q+1/2}(\rho) \tag{117}$$

$$T_{\rho c}^{n}(\rho) = \frac{2d}{\rho} \sum_{q=1}^{M-1} v_{\rho q}^{n\perp} P_{q+1/2}(\rho) \quad n=1,2,\ldots,N \tag{118}$$

$$T_{\phi s}^{n}(\rho) = 2j \sum_{q=1}^{M} v_{\phi q}^{n\perp} P_{q}(\rho) \quad n=1,2,\ldots,N \tag{119}$$

Notice the symmetry,

$$\bar{v}_{\rho}^{-n\perp} = \bar{v}_{\rho}^{n\perp} \tag{120}$$

$$\bar{v}_{\phi}^{-n\perp} = -\bar{v}_{\phi}^{n\perp} \tag{121}$$

which can be seen from (103), (106) and (107).

(ii) $E_{/\!/}$-Polarization

Similarly, from (30), (44), (45) and (62), we can obtain, for this polarization,

$$I_{\rho q}^{n} = E^{io}\, i_{\rho q}^{n/\!/} \tag{122}$$

$$I_{\phi q}^{n} = E^{io}\, i_{\phi q}^{n/\!/} \tag{123}$$

where

$$i_{\rho q}^{n/\!/} = -\, i_{\rho q}^{-n/\!/} = \frac{1}{\eta_o}\, j^{-n}[J_{n+1}(\beta x_q) + J_{n-1}(\beta x_q)] \tag{124}$$

$$i_{\phi q}^{n/\!/} = i_{\phi q}^{-n/\!/} = \frac{-1}{\eta_o}\, j^{-n+1}\, x_{q-1/2}[J_{n+1}(\beta x_{q-1/2}) - J_{n-1}(\beta x_{q-1/2})] \tag{125}$$

and a column matrix

$$\bar{v}^{n/\!/} = \begin{bmatrix} \bar{v}_{\rho}^{n/\!/} \\ \bar{v}_{\phi}^{n/\!/} \end{bmatrix} = \begin{bmatrix} \begin{bmatrix} v_{\rho 1}^{n/\!/} \\ \vdots \\ v_{\rho M-1}^{n/\!/} \end{bmatrix} \\ \begin{bmatrix} v_{\phi 1}^{n/\!/} \\ \vdots \\ v_{\phi M}^{n/\!/} \end{bmatrix} \end{bmatrix} \tag{126}$$

is introduced as the solution of the equation

$$\tilde{\bar{Y}}^{n}\ \bar{v}^{n''} = \bar{i}^{n''} \tag{127}$$

where

$$\bar{i}^{n''} = \begin{bmatrix} \bar{i}^{n''}_{\rho} \\ \bar{i}^{n''}_{\phi} \end{bmatrix} = \begin{bmatrix} \begin{bmatrix} i^{n''}_{\rho 1} \\ \vdots \\ i^{n''}_{\rho M-1} \end{bmatrix} \\ \begin{bmatrix} i^{n''}_{\phi 1} \\ \vdots \\ i^{n''}_{\phi M} \end{bmatrix} \end{bmatrix} \tag{128}$$

The magnetic current in this case can be written as

$$\underline{M}_{o} = E^{io}(m''_{\rho}\ \underline{\hat{u}} + m''_{\phi}\ \underline{\hat{u}}_{\phi}) \tag{129}$$

where

$$m''_{\rho} = \sum_{n=1}^{N} T^{n}_{\rho s}(\rho)\ \sin n\phi \tag{130}$$

$$m''_{\phi} = T^{o}_{\phi}(\rho) + \sum_{n=1}^{N} T^{n}_{\phi c}(\rho)\ \cos n\phi \tag{131}$$

$$T^{n}_{\rho s}(\rho) = \frac{2jd}{\rho} \sum_{q=1}^{M-1} v^{n''}_{\rho q}\ P_{q+1/2}(\rho) \qquad n=1,2,\ldots,N \tag{132}$$

$$T^{o}_{\phi}(\rho) = \sum_{q=1}^{M} v^{o''}_{\phi q}\ P_{q}(\rho) \tag{133}$$

$$T^{n}_{\phi c}(\rho) = 2 \sum_{q=1}^{M} v^{n''}_{\phi q}\ P_{q}(\rho) \qquad n=1,2,\ldots,N \tag{134}$$

The symmetry used in this case is

$$\bar{v}^{-n''}_{\rho} = -\ \bar{v}^{n''}_{\rho} \tag{135}$$

$$\bar{v}^{-n''}_{\phi} = \bar{v}^{n''}_{\phi} \tag{136}$$

V. GAIN PATTERN AND TRANSMISSION COEFFICIENT

Formulas for the two transmission characteristics are given here in terms of the magnetic current coefficients.

(a) Power Gain Pattern on the Transmitted Side

The power gain pattern $G(\theta,\phi)$ on the transmitted side is defined as

$$G(\theta,\phi) = \pi r^2 \frac{k^2}{\eta_o} [|F_\phi|^2 + |F_\theta|^2]/P_t \tag{137}$$

where F_ϕ, F_θ are components of the vector potential $\underline{F}$,

$$\underline{F} = \frac{e^{-jkr}}{2\pi r} \iint_{\text{aperture}} \underline{M}_o(\underline{r}')e^{-jkr'\cos\xi} da' \tag{138}$$

in the far zone and

$$\cos\xi = \cos\theta\cos\theta' + \sin\theta\sin\theta'\cos(\phi' - \phi) \tag{139}$$

while $(r,\theta,\phi),(r',\theta',\phi')$ denote the field point and source point, respectively.

P_t is the time average of the total power transmitted through the aperture and is given by,

$$P_t = \frac{1}{2} \iint_{\text{aperture}} \text{Re}(\underline{\hat{n}} \cdot \underline{E}^* \times \underline{H})\, da \tag{140}$$

or,

$$P_t = \frac{1}{2} \iint_{\text{aperture}} \text{Re}(\underline{M}^* \cdot \underline{H})\, da \tag{141}$$

From (2), (8) and (141), we obtain

$$P_t = \operatorname{Re} \sum_{ij} V_i^* V_j \langle \underline{M}_i^*, \tilde{\underline{H}}(\underline{M}_j) \rangle \tag{142}$$

From Section III-(a), we notice that when the subsections are small, $\underline{M}_i^*$ in (142) can be approximated by $\underline{W}_i^*$ with a constant factor and an approximate expression for P_t is obtained,

$$P_t = \operatorname{Re} \{ \frac{\pi\Delta^2}{2} \sum_{n=-N}^{N} [\sum_{q=1}^{M-1} M \, V_{\rho q}^{n*} \, I_{\rho q}^{n} + \sum_{q=1}^{M} V_{\phi q}^{n*} \, I_{\phi q}^{n}] \} \tag{143}$$

From (104), (105), (112) and (143), we obtain, for the $E_\perp$-polarization,

$$P_t = \frac{1}{2} \operatorname{Re} \{ |E^{io}|^2 \pi\Delta^2 \sum_{n=0}^{N} \varepsilon_n \begin{bmatrix} M \, \bar{v}_\rho^{n\perp} \\ \\ \bar{v}_\phi^{n\perp} \end{bmatrix}^{*T} \bar{i}^{n\perp} \} \tag{144}$$

where $\varepsilon_n = 1$ for $n = 0$ and $\varepsilon_n = 2$ for $n \geq 1$. From (122), (123), (127) and (143), we obtain, for the $E_{/\!/}$-polarization

$$P_t = \frac{1}{2} \operatorname{Re} \{ |E^{io}|^2 \pi\Delta^2 \sum_{n=0}^{N} \varepsilon_n \begin{bmatrix} M \, \bar{v}_\rho^{n/\!/} \\ \\ \bar{v}_\phi^{n/\!/} \end{bmatrix}^{*T} \bar{i}^{n/\!/} \} \tag{145}$$

Another method for calculating P_t is to integrate the far field radiation:

$$P_t = \frac{k^2}{2\eta_o} \int_0^{\pi/2} r^2 \sin\theta \, d\theta \int_0^{2\pi} [|F_\phi|^2 + |F_\theta|^2] d\phi \tag{146}$$

The ϕ-integration in Eq. (146) is trivial because of the orthogonality of the trigonometric functions. The θ-integration is done by quadratures.

F_ϕ, F_θ used in (137) and (146) are given in terms of the magnetic current coefficients in two separate polarizations:

(i) $E_\perp$-polarization

For incident fields defined by (40) and (41) with $\hat{\underline{u}}_e = \hat{\underline{u}}_\perp$, substitute (115) to (119) into (138), assume the condition of (79), and obtain

$$F_\phi = E^{io} f_\phi^\perp \tag{147}$$

$$F_\theta = E^{io} f_\theta^\perp \tag{148}$$

where

$$f_\phi^\perp = \frac{\Delta^2 e^{-jkr}}{r} \sum_{n=1}^{N} \sin n\phi \{ j^{n+1} M \sum_{q=1}^{M-1} v_{\rho q}^{n\perp} [J_{n+1}(\kappa x_q \sin\theta) + J_{n-1}(\kappa x_q \sin\theta)]$$

$$- j^n \sum_{q=1}^{M} v_{\phi q}^{n\perp} [x_{q-1/2}(J_{n+1}(\kappa x_{q-1/2} \sin\theta) - J_{n-1}(\kappa x_{q-1/2} \sin\theta))$$

$$+ \frac{\kappa \sin\theta}{24} (2J_n(\kappa x_{q-1/2} \sin\theta) - J_{n+2}(\kappa x_{q-1/2} \sin\theta)$$

$$- J_{n-2}(\kappa x_{q-1/2} \sin\theta))]\} \tag{149}$$

$$f_\theta^\perp = \frac{\Delta^2 e^{-jkr}}{2r} \cos\theta \sum_{n=0}^{N} \varepsilon_n \cos n\phi \{ j^{n+1} M \sum_{q=1}^{M-1} v_{\rho q}^{n\perp} [J_{n+1}(\kappa x_q \sin\theta) - J_{n-1}(\kappa x_q \sin\theta)]$$

$$-j^n \sum_{q=1}^{M} v_{\phi q}^{n\perp} [x_{q-1/2}(J_{n+1}(\kappa x_{q-1/2} \sin\theta) + J_{n-1}(\kappa x_{q-1/2} \sin\theta))$$

$$- \frac{\kappa \sin\theta}{24} (J_{n+2}(\kappa x_{q-1/2} \sin\theta) - J_{n-2}(\kappa x_{q-1/2} \sin\theta))]\} \tag{150}$$

and $\varepsilon_n = 1$ for $n = 0$ and $\varepsilon_n = 2$ for $n \neq 0$

(ii) $E_{\parallel}$-polarization

For incident fields defined by (40) and (41) with $\underline{\hat{u}}_e = \underline{\hat{u}}_{\parallel}$, substitute (130) to (134) into (138), assume the condition of (79), and obtain

$$F_\phi = E^{io} f_\phi^{\parallel} \tag{151}$$

$$F_\theta = E^{io} f_\theta^{\parallel} \tag{152}$$

where

$$\begin{aligned} f_\phi^{\parallel} = \frac{\Delta^2 e^{-jkr}}{2r} \sum_{n=0}^{N} \varepsilon_n \cos n\phi \{ & j^n M \sum_{q=1}^{M-1} v_{\rho q}^{n\parallel} [J_{n+1}(\kappa x_q \sin\theta) + J_{n-1}(\kappa x_q \sin\theta)] \\ & + j^{n+1} \sum_{q=1}^{M} v_{\phi q}^{n\parallel} [x_{q-1/2}(J_{n+1}(\kappa x_{q-1/2}\sin\theta) - J_{n-1}(\kappa x_{q-1/2}\sin\theta)) \\ & + \frac{\kappa \sin\theta}{24}(2J_n(\kappa x_{q-1/2}\sin\theta) - J_{n+2}(\kappa x_{q-1/2}\sin\theta) \\ & - J_{n-2}(\kappa x_{q-1/2}\sin\theta))]\} \end{aligned} \tag{153}$$

$$\begin{aligned} f_\theta^{\parallel} = \frac{\Delta^2 e^{-jkr}}{r} \sum_{n=1}^{N} \sin n\phi \{ & -j^n M \sum_{q=1}^{M-1} v_{\rho q}^{n\parallel} [J_{n+1}(\ x_q \sin\theta) - J_{n-1}(\kappa x_q \sin\theta)] \\ & - j^{n+1} \sum_{q=1}^{M} v_{\phi q}^{n\parallel} [x_{q-1/2}(J_{n+1}(\kappa x_{q-1/2}\sin\theta) + J_{n-1}(\kappa x_{q-1/2}\sin\theta)) \\ & - \frac{\kappa \sin\theta}{24}(J_{n+2}(\kappa x_{q-1/2}\sin\theta) - J_{n-2}(\kappa x_{q-1/2}\sin\theta))]\} \end{aligned} \tag{154}$$

(b) <u>Transmission Coefficient</u>

The transmission coefficient is defined as the ratio,

$$TC = \frac{P_t}{P_{in}} \tag{155}$$

where P_t is defined in the last section and P_{in} is the time average of

the total power incident upon the aperture by the incident sources when the incidence is normal. It is given by,

$$P_{in} = \frac{|E^{io}|^2}{2\eta_o} \pi(R_{out}^2 - R_{in}^2) \tag{156}$$

or

$$P_{in} = \frac{|E^{io}|^2}{2\eta_o} \pi\Delta^2 M(M + 2x_o) \tag{157}$$

VI. NUMERICAL RESULTS AND DISCUSSION

Numerical results for a number of cases are given in this section. Several examples are given first with normal incident waves where only the n=1 mode is needed and only one polarization needs to be considered. $E_\perp$-polarization is chosen for these examples. The results for the other polarization are easily obtained from this polarization. Results for oblique incidences are illustrated for two typical apertures (one small and one intermediate). Both polarizations are considered and an adequate number of modes are used.

In the figures showing results for the magnetic currents, points are plotted according to the actual representation at the centers of each subsection (ρ-component is marked by symbol Δ, ϕ- component is marked by symbol ⊡). Note that subsections for the two polar components are shifted from each other by $\frac{\Delta}{2}$. Points are then connected by straight line segments. At $\rho = R_{out}$, the value zero is plotted for the ρ-component corresponding to the boundary condition. At $\rho = R_{in}$, except for the case when $R_{in} = 0$ and $n = \pm 1$, the value of the ρ-component should also go to zero. This is discussed in previous work [5]. For the exception just

mentioned, no value is plotted at $\rho = R_{in}$.

The power gain patterns are computed in both the E-plane and the H-plane at elevation angles one degree apart. The transmission coefficient is computed for both $E_\perp$ and $E_{\parallel}$- polarization at angles of incidence 15° apart.

Figure 3 shows both components of the magnetic currents for normal incidence on an aperture with $R_{out} = .05\lambda$, while R_{in} varies from 0 to $.01\lambda$ to $.03\lambda$. Figures 4 to 6 show both components of the magnetic currents for circular apertures of sizes $R_{out} = .25\lambda$, $.5\lambda$ and 1.5λ respectively.

These results (Figs. 4-6) were compared with previous work [7]. Better convergence is observed for the first two cases, while in the third case ($R_{out} = 1.5\lambda$), our result is quite different from theirs and seems to be more accurate.

In Figs. 7 to 11, results for oblique incidences on a small aperture ($R_{out} = .02\lambda$, $R_{in} = 0$) are shown. For this small an aperture, the n=1 mode dominates for $E_\perp$-incidence, while both n=0 and n=1 modes are important for $E_{\parallel}$-incidence. This result can be seen from examining the Bessel functions and the matrix elements. Both components of n=1 mode are shown for $E_\perp$ -polarization and for a number of angles of incidence in Figs. 7, 8. Figures 10, 11 are the equivalences of Figs. 7, 8 for $E_{\parallel}$- polarization while Fig. 9 shows the circulating current (n=0 mode) for this polarization.

Gain patterns for this aperture are also computed. For $E_\perp$- polarization, a simple dipole pattern is observed. A change in the

angle of incidence only changes the magnitude of the dipole (the n=1 mode) and doesn't change the pattern shape. These simple dipole patterns are not shown, since they are well known. For $E_{//}$-polarization, since both dipoles exist (the n=0 and n=1 modes), the patterns are more complicated and are shown for a number of oblique incidences in both planes in Figs. 18 and 19.

In Figs. 12 to 17, magnetic currents for oblique incidences on an aperture of medium size ($R_{out} = .25\lambda$, $R_{in} = 0$) are shown. At 45° incidence, the magnitudes of the first few dominant modes are compared for both components and for both polarizations. The same is done for 90° incidence, except in this case $E_{\perp}$ -polarization doesn't excite the aperture.

Gain patterns for oblique incidences on this aperture are shown in Figs. 20 to 23, again, for both E and H-planes and for both polarizations.

The transmission coefficients versus angle of incidence are plotted in Figs. 24 and 25 for the two apertures, both polarizations considered. For the case where $R_{out} = .02\lambda$, the result compare very well with formulas by Bethe [6]. A slower convergence than that for the currents was observed, and the pulse representation of the edge behavior of the ϕ-component of the current is considered the reason for this.

Power gain patterns shown in the figures are normalized with respect to the maximum gain in each particular plane. Table 1 retains the information needed when these patterns are normalized.

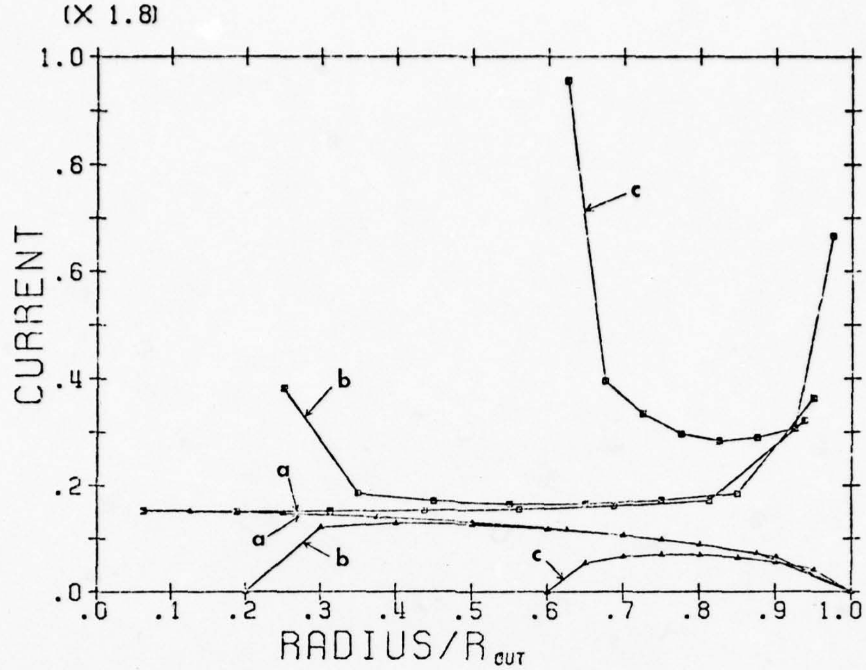

Fig. 3. First mode, ρ and ϕ components of magnetic current, $-jT^1_{\rho c}$ and $J^1_{\phi s}$, for apertures of $R_{out} = .05\lambda$. (a) $R_{in} = 0$, (b) $R_{in} = .01\lambda$, (c) $R_{in} = .03\lambda$. Normal incidence.

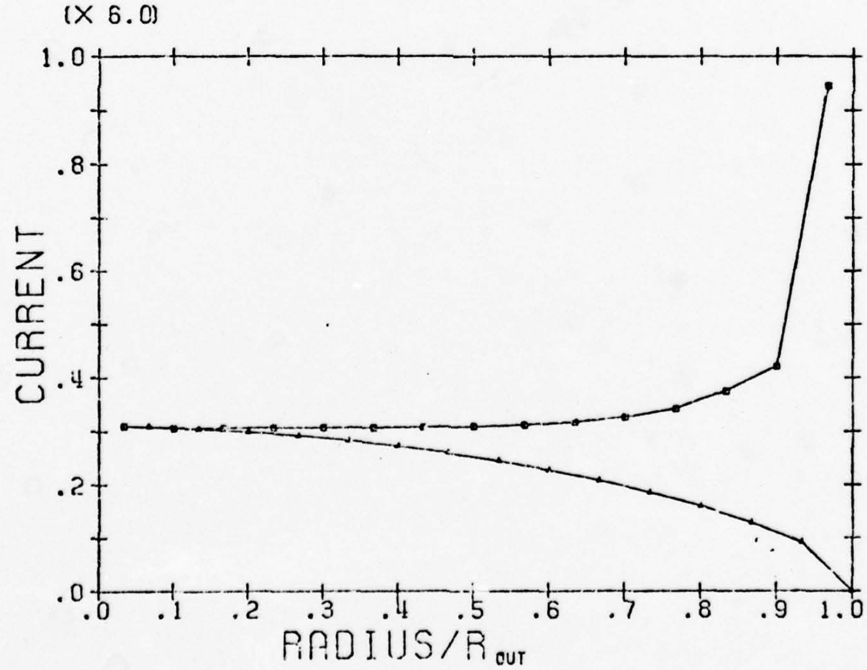

Fig. 4. First mode, ρ and ϕ components of magnetic current, $|T^1_{\rho c}|$ and $|T^1_{\phi s}|$, for a circular aperture of $R_{out} = .25\lambda$, normal incidence.

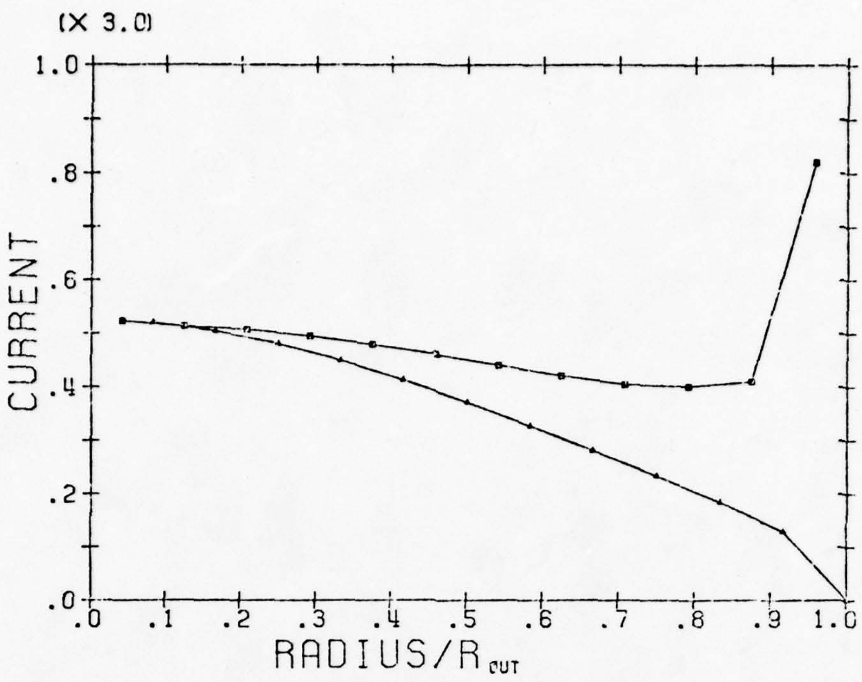

Fig. 5. First mode, ρ and ϕ components of magnetic current, $|T^1_{\rho c}|$ and $|T^1_{\phi s}|$ for a circular aperture of R_{out} = .5λ,normal incidence.

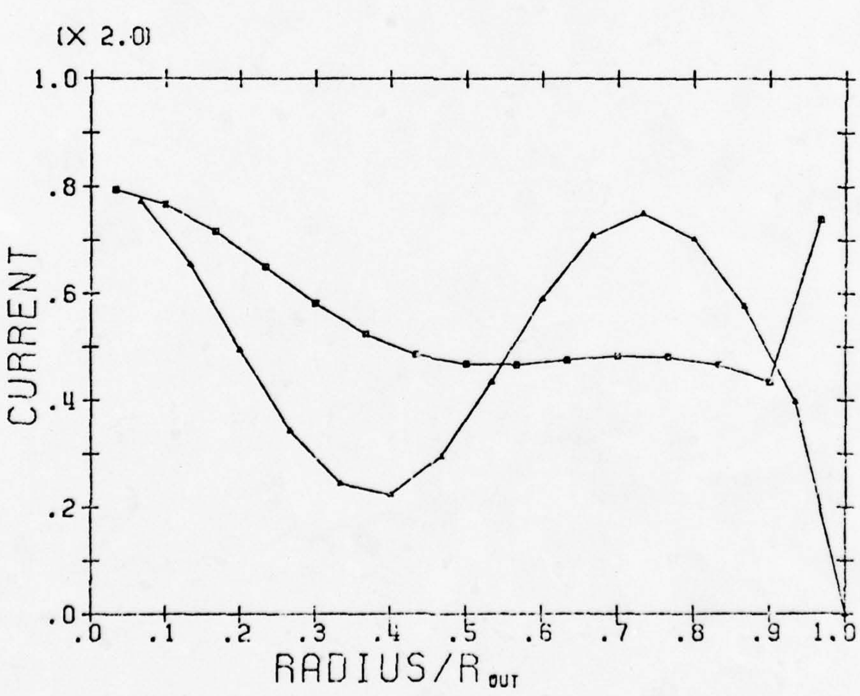

Fig. 6. First mode, ρ and ϕ components of magnetic current, $|T^1_{\rho c}|$ and $|T^1_{\phi s}|$ for a circular aperture of R_{out} = 1.5λ, normal incidence.

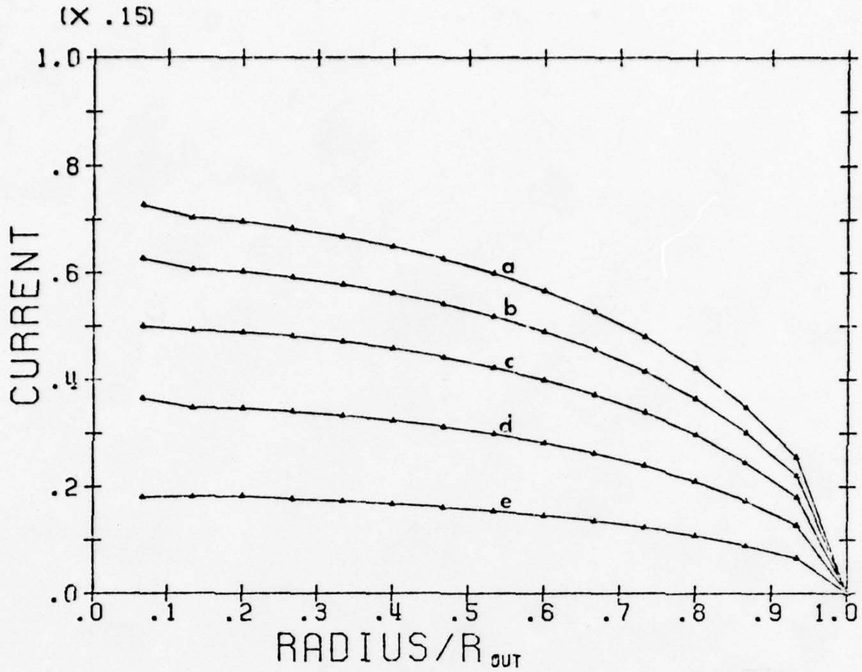

Fig. 7. First mode, ρ component of magnetic current for $E_{\perp}$-polarization, $-jT^{1}_{\rho c}$ for a circular aperture of $R_{out} = .02\lambda$, angles of incidence (a) 0°, (b) 30°, (c) 45°, (d) 60° and (e) 75°.

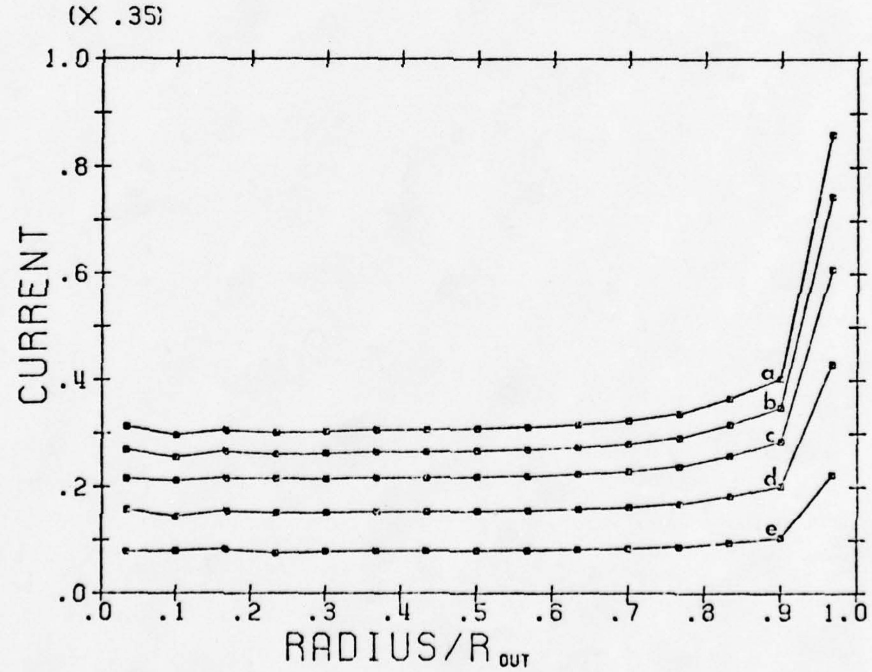

Fig. 8. First mode, φ component of magnetic current for $E_{\perp}$-polarization, $jT^{1}_{\rho s}$, for a circular aperture of $R_{out} = .02\lambda$, angles of incidence (a) 0°, (b) 30°, (c) 45°, (d) 60° and (e) 75°.

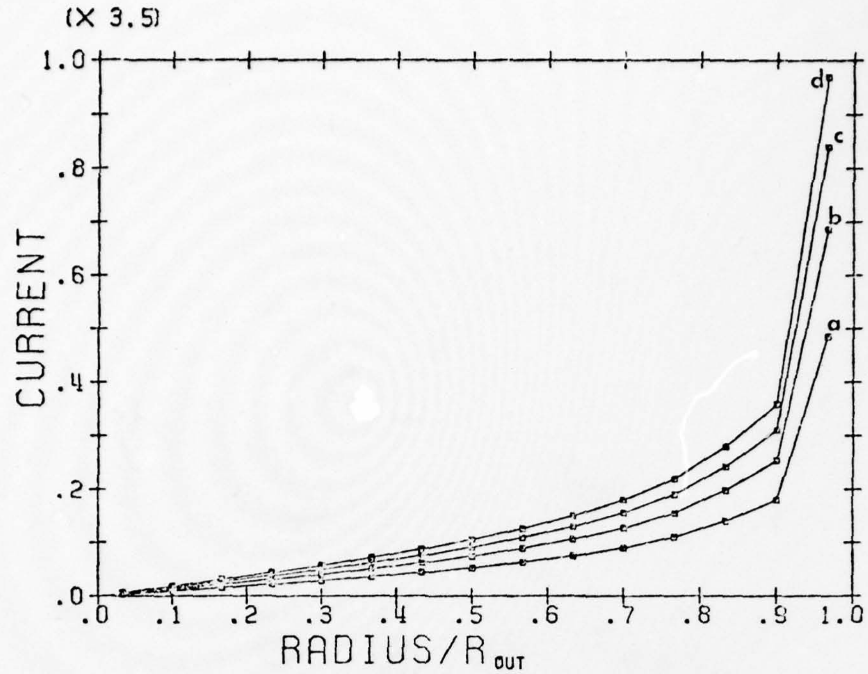

Fig. 9. Zeroth mode, ϕ component of magnetic current for E - polarization, $-T^{o}_{\phi}$, for a circular aperture of R_{out} = .02λ, angles of incidence (a) 30°, (b) 45°, (c) 60°, and (d) 90°.

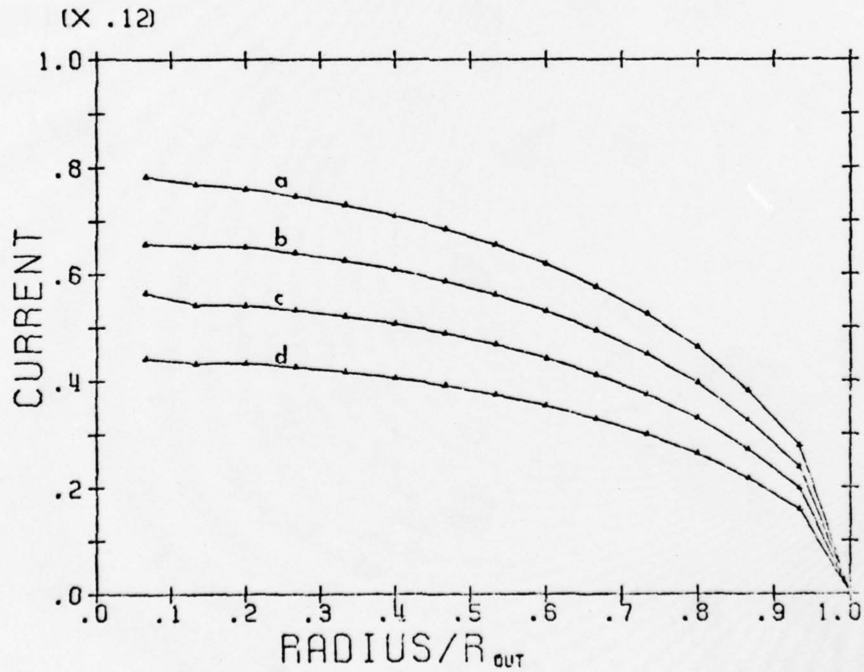

Fig. 10. First mode, ρ component of magnetic current for $E_{\parallel}$ - polarization, $jT^{1}_{\rho s}$, for a circular aperture of R_{out} = .02λ, angles of incidence (a) 30°, (b) 45°, (c) 60° and (d) 90°.

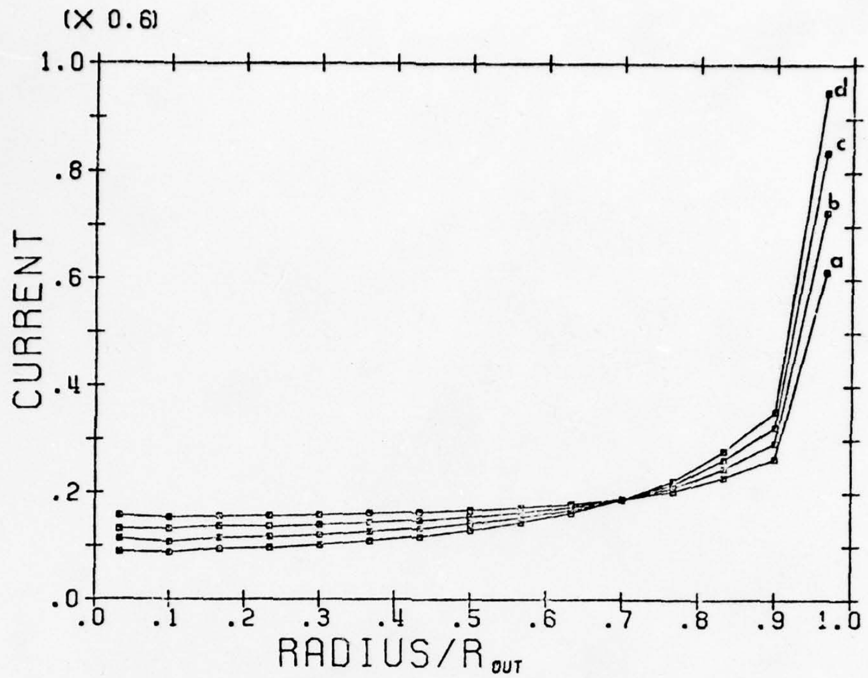

Fig. 11. First mode, ϕ component of magnetic current for $E_{\parallel}$ -polarization, $jT^{1}_{\phi c}$, for a circular aperture of R_{out} = .02λ, angles of incidence (a) 30°, (b) 45°, (c) 60° and (d) 90°.

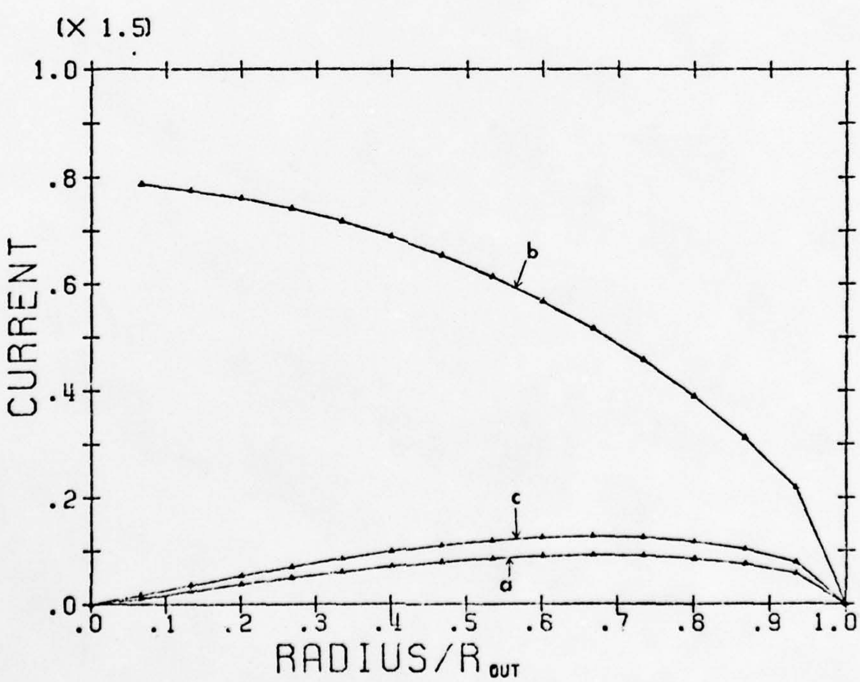

Fig. 12. Zeroth, first and second mode, ρ component of magnetic current for $E_{\perp}$-polarization (a) $|T^{o}_{\rho}|$,(b) $|T^{1}_{\rho c}|$, and (c) $|T^{2}_{\rho c}|$, for a circular aperture of R_{out} = .25λ, 45° incidence.

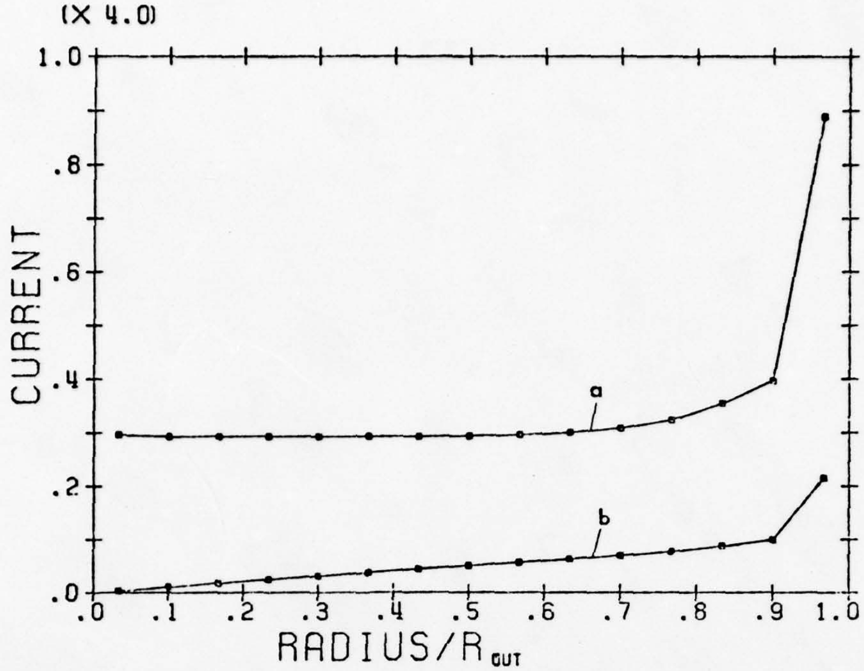

Fig. 13. First and second mode, ϕ component of magnetic current for $E_\perp$ - polarization, (a) $|T^1_{\phi s}|$, (b) $|T^2_{\phi s}|$, for a circular aperture of R_{out} = .25λ, 45° incidence.

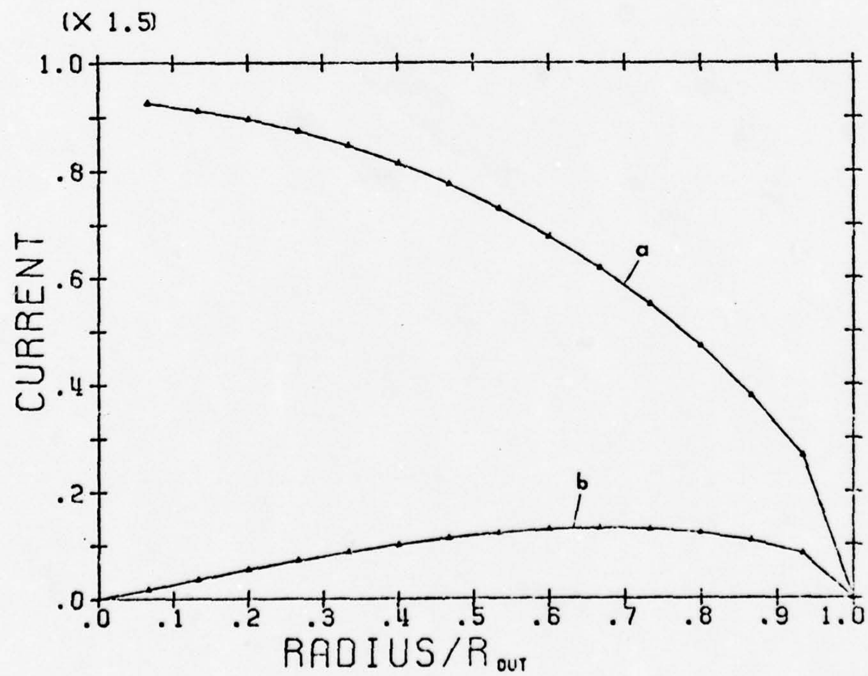

Fig. 14. First and second mode, ρ component of magnetic current for $E_{/\!/}$ -polarization, (a) $|T^1_{\rho s}|$, (b) $|T^2_{\rho s}|$, for a circular aperture of R_{out} = .25λ, 45° incidence.

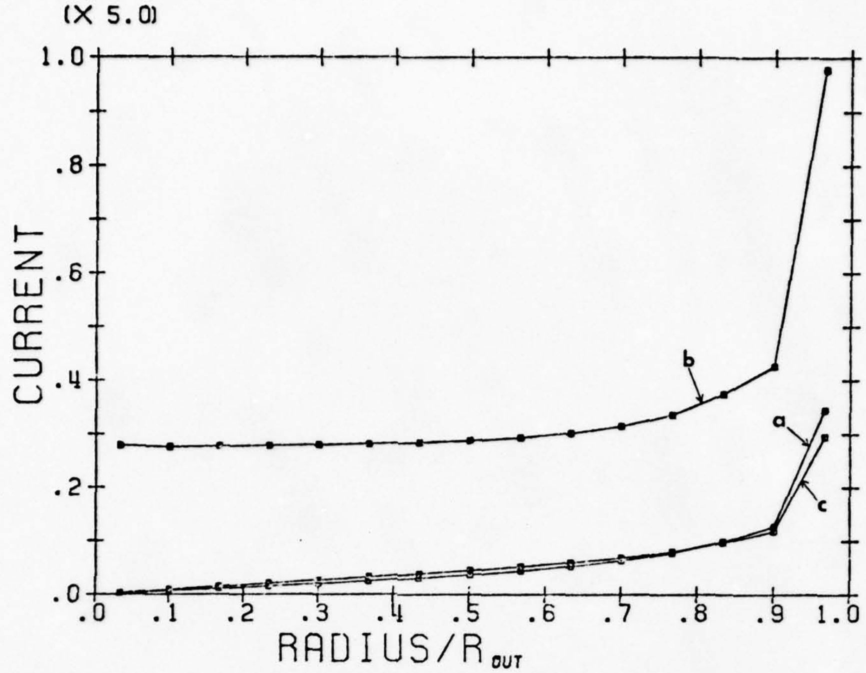

Fig. 15. Zeroth, first and second mode, ϕ component of magnetic current for $E_{\parallel}$ -polarization, (a) $T^{o}_{\phi}|$, (b) $|T^{1}_{\phi c}|$, and (c) $|T^{2}_{\phi c}|$, for a circular aperture of $R_{out} = .25\lambda$, 45° incidence.

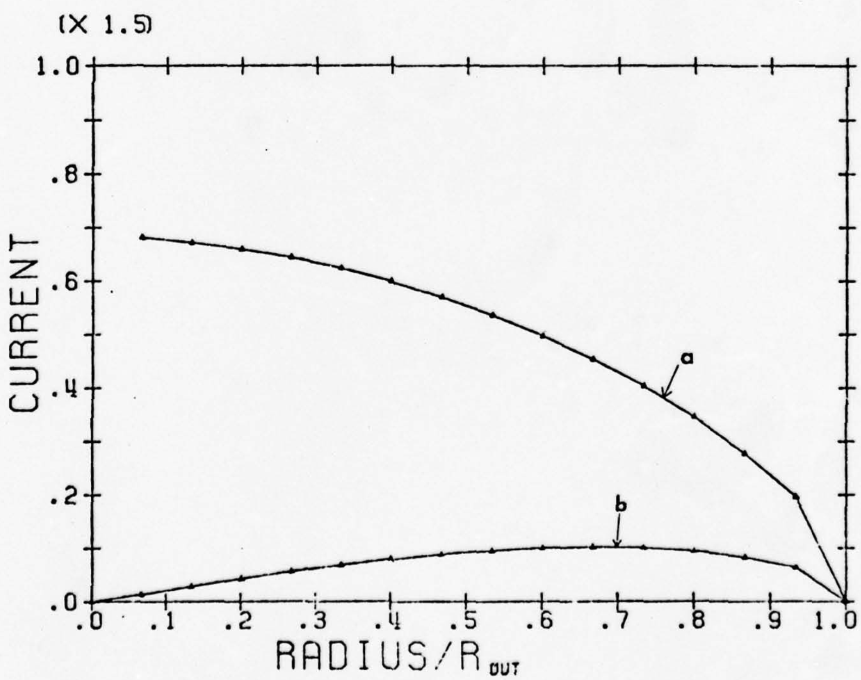

Fig. 16. First and second mode, ρ component of magnetic current for $E_{\parallel}$ - polarization, (a) $|T^{1}_{\rho s}|$, (b) $|T^{2}_{\rho s}|$, for a circular aperture of $R_{out} = .25\lambda$, 90° incidence.

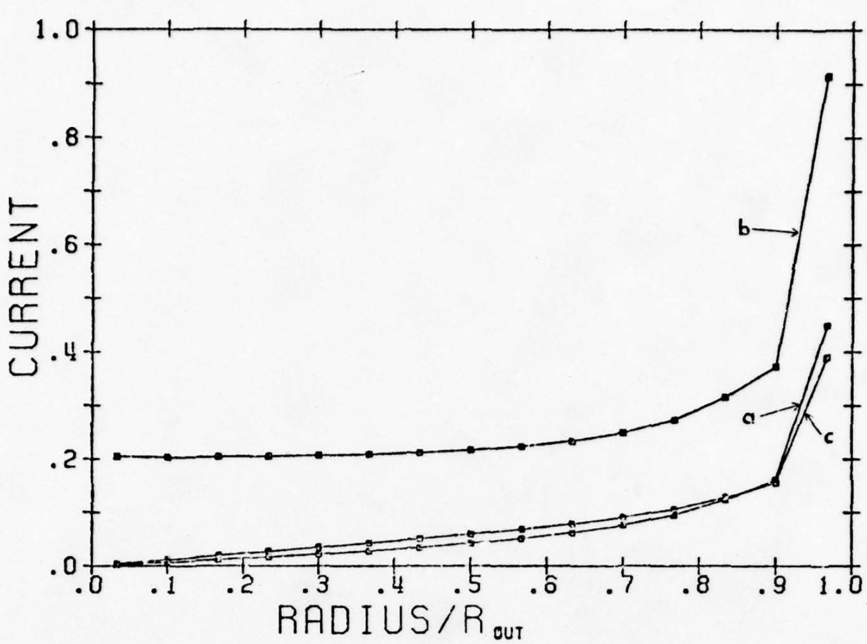

Fig. 17. Zeroth, first and second mode, ϕ component of magnetic current for $E_{/\!/}$-polarization, (a) $|T_{\phi}^{o}|$, (b) $|T_{\phi c}^{1}|$, and (c) $|T_{\phi c}^{2}|$, for a circular aperture of R_{out} = .25λ, 90° incidence.

Curve	$G(\theta_{max})$	θ_{max}	Curve	$G(\theta_{max})$	θ_{max}
18-(a)	1.874	90°	21-(a)	2.358	0°
-(b)	2.195	90°	-(b)	2.345	3°
-(c)	2.430	90°	-(c)	2.331	4°
-(d)	2.581	90°	-(d)	2.323	5°
-(e)	2.662	90°	22-(a)	2.312	2°
-(f)	2.687	90°	-(b)	2.191	4°
19-(a)	1.480	0°	-(c)	2.111	4°
-(b)	1.341	0°	23-(a)	2.309	0°
-(c)	1.225	0°	-(b)	2.184	0°
20	2.331	0°	-(c)	2.102	0°

Table 1. Maximum gains in each normalized gain patterns and elevation angles at which they occur.

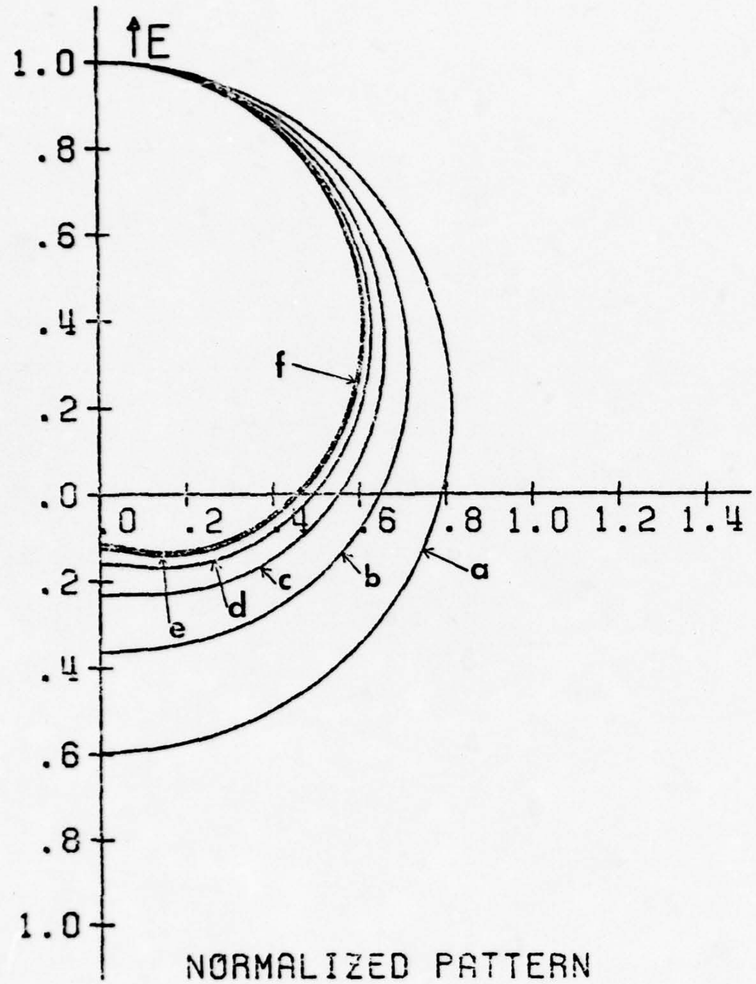

Fig. 18. Normalized gain pattern in the E-plane for a circular aperture of $R_{out} = .02\lambda$, for $E_{/\!/}$-polarization, angles of incidence (a) 15°, (b) 30°, (c) 45°, (d) 60°, (e) 75° and (f) 90°.

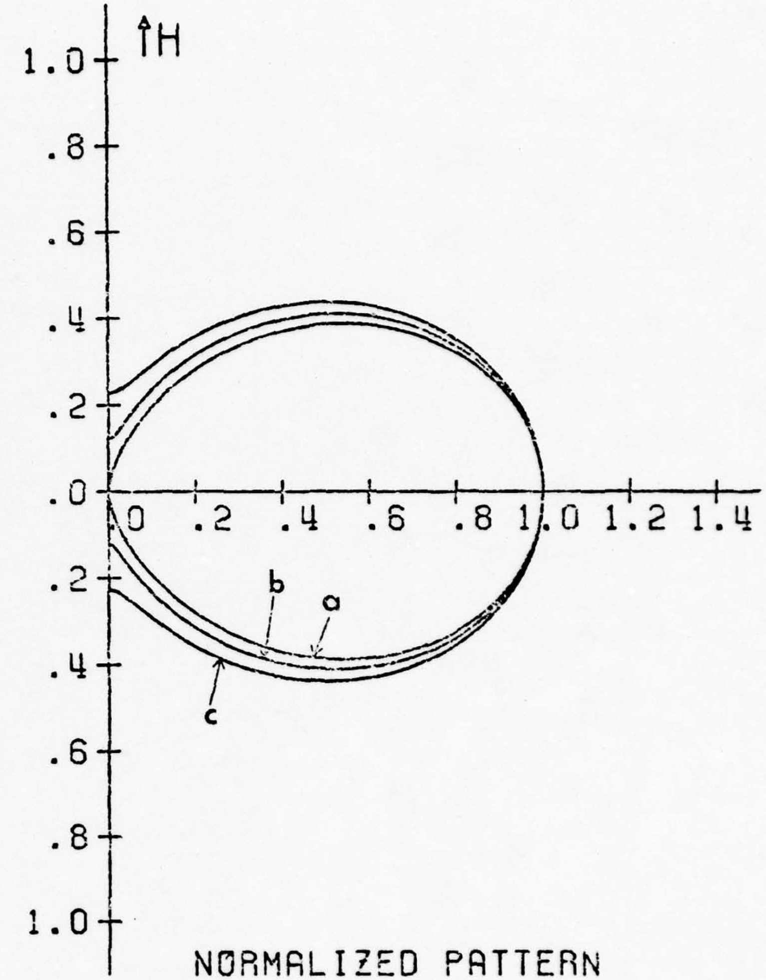

Fig. 19. Normalized gain pattern in the H-plane for a circular aperture of $R_{out} = .02\lambda$, for $E_{/\!/}$-polarization, angles of incidence (a) 15°, (b) 45°, and (c) 75°.

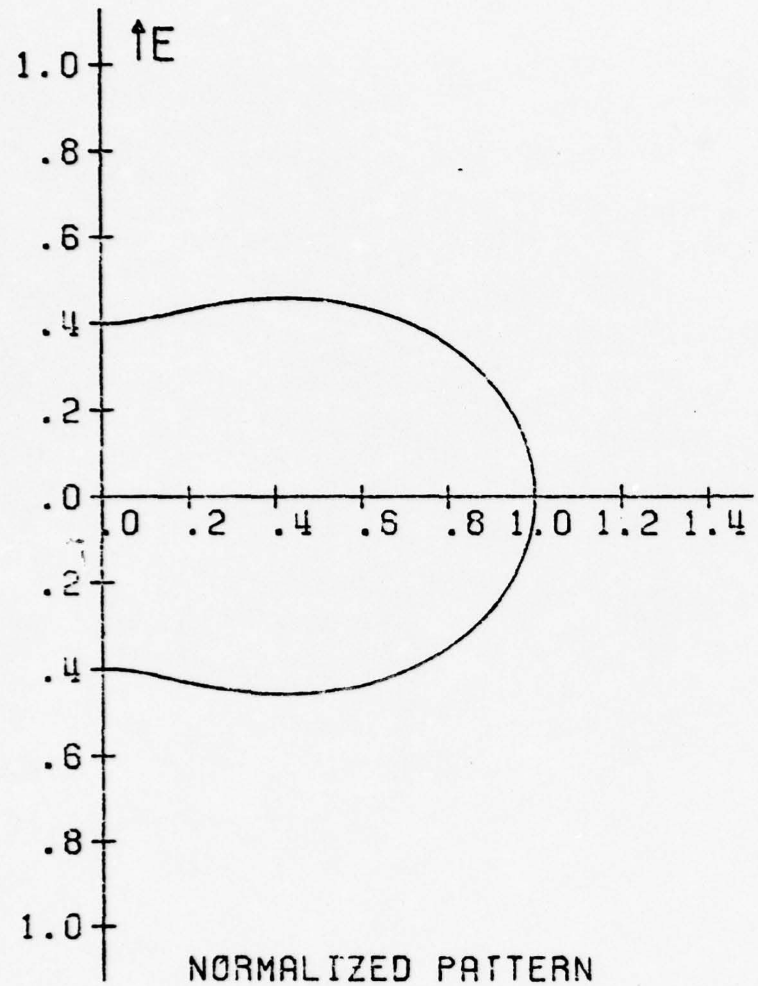

Fig. 20. Normalized gain pattern in the E-plane for a circular aperture of $R_{out} = .25\lambda$, for $E_\perp$-polarization. All angles of incidence produce the same pattern.

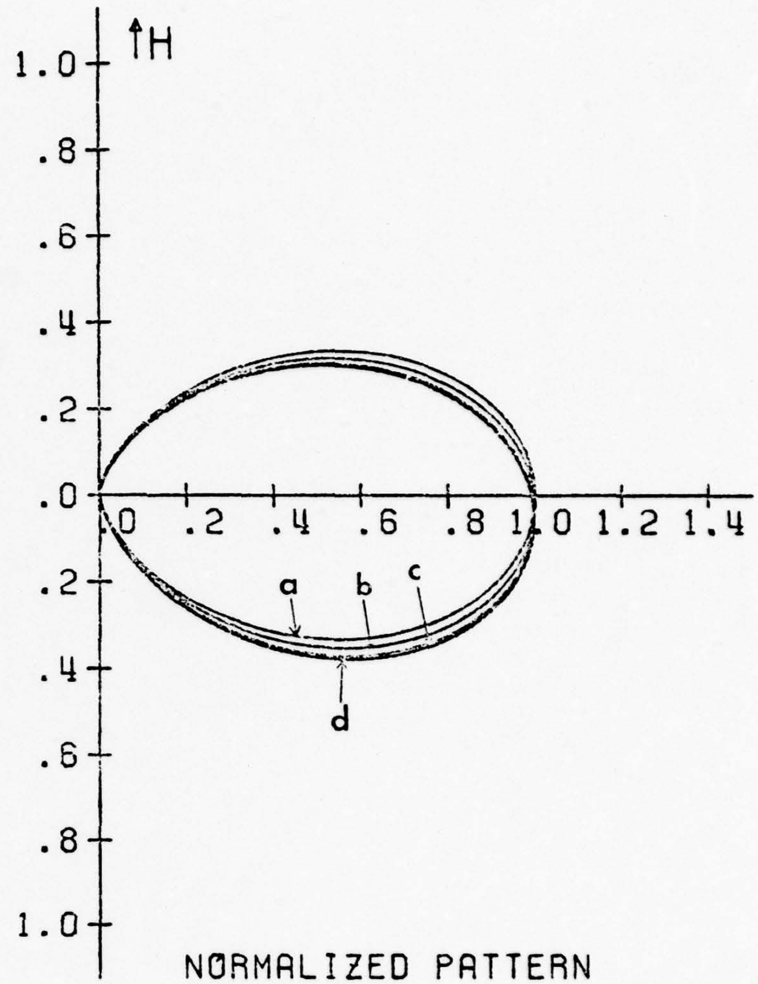

Fig. 21. Normalized gain pattern in the H-plane for a circular aperture of $R_{out} = .25\lambda$, for $E_\perp$-polarization, angles of incidence (a) 0°, (b) 30°, (c) 60°, and (d) 75°.

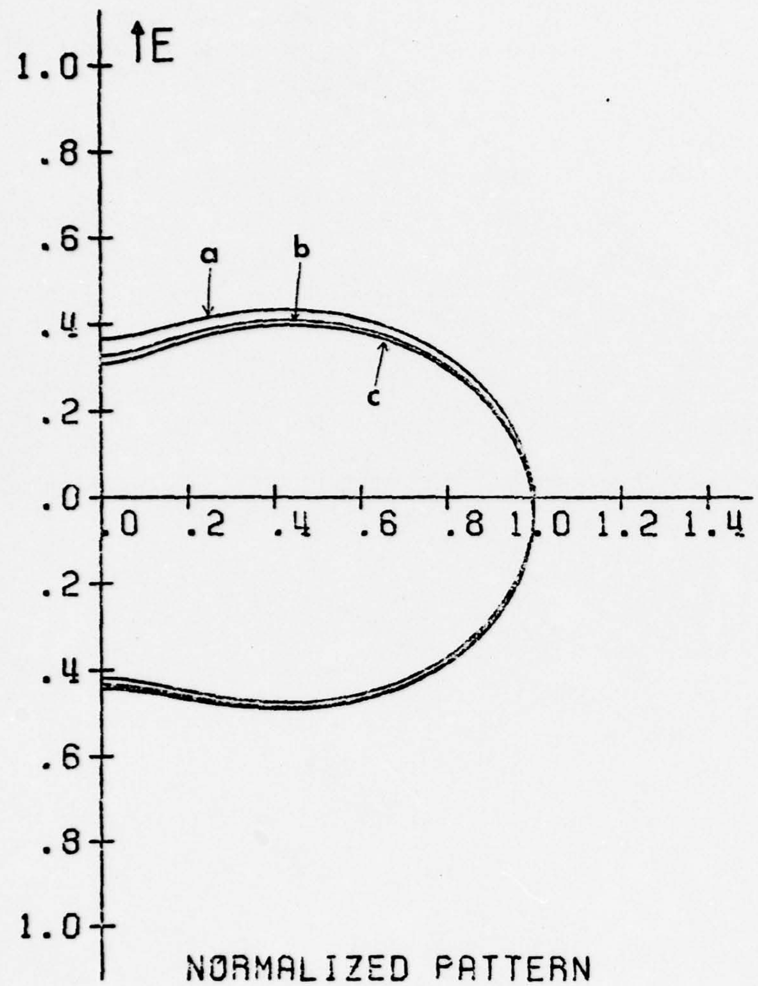

Fig. 22. Normalized gain pattern in the E-plane for a circular aperture of $R_{out} = .25\lambda$, for $E_{\parallel}$ -polarization, angles of incidence (a) 30°, (b) 60°, and (c) 90°.

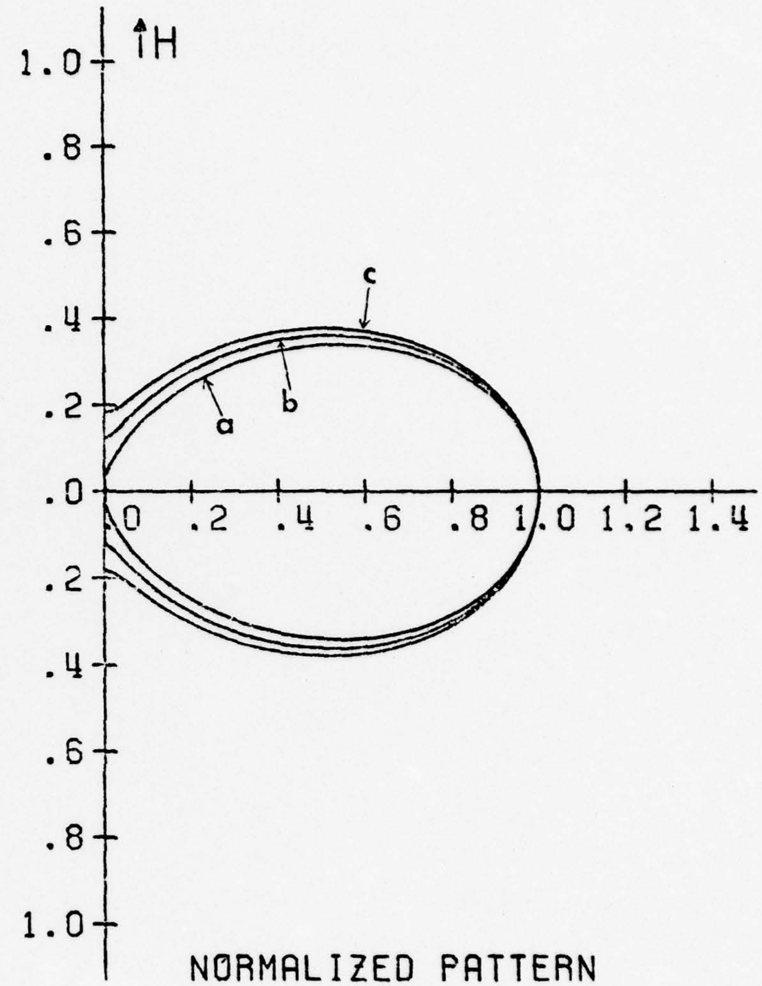

Fig. 23. Normalized gain pattern in the H-plane for a circular aperture of $R_{out} = .25\lambda$, for $E_{\parallel}$ -polarization, angle of incidence (a) 30°, (b) 60°, (c) 90°.

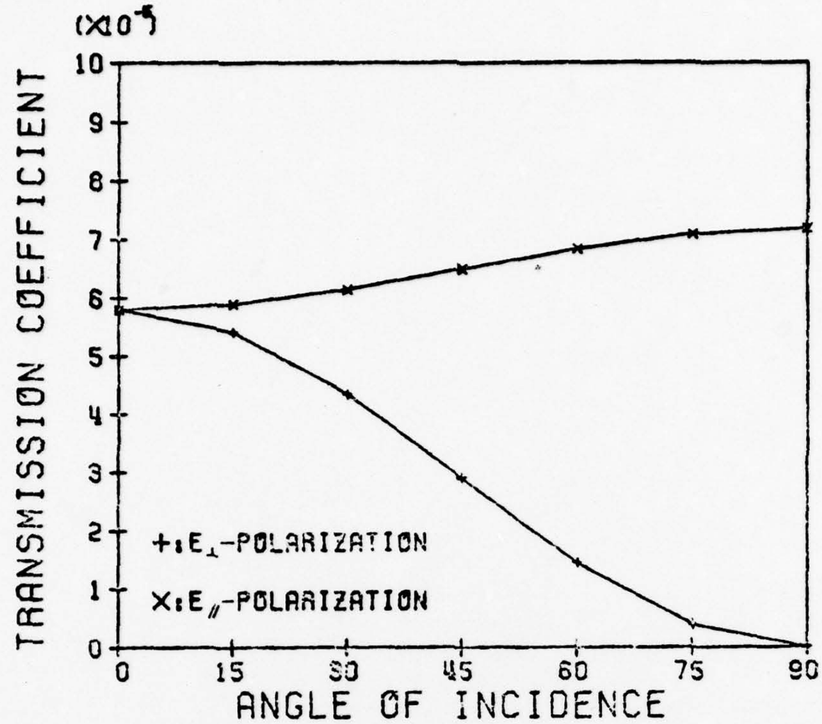

Fig. 24. Transmission coefficient for a circular aperture of $R_{out} = .02\lambda$.

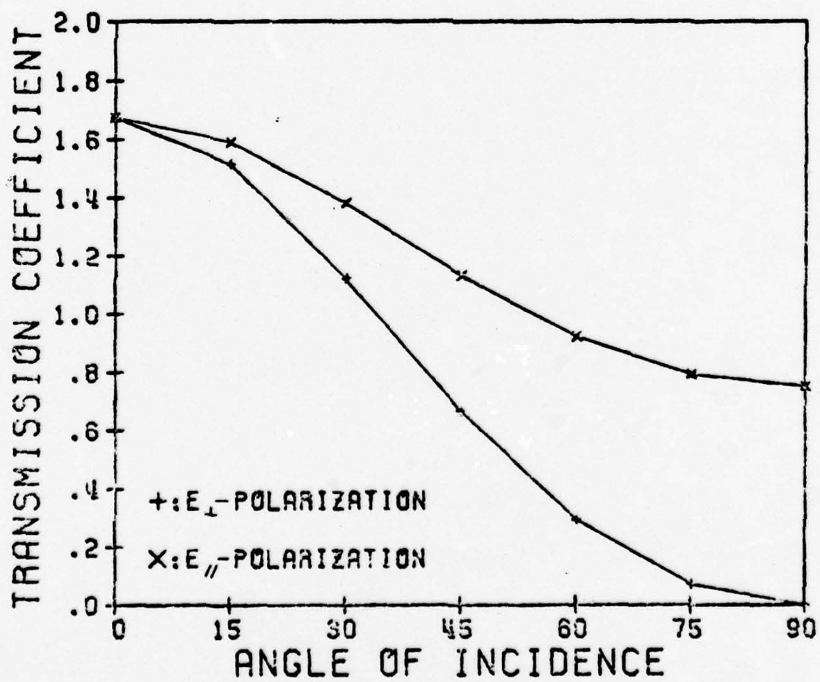

Fig. 25. Transmission coefficient for a circular aperture of $R_{out} = .25\lambda$.

VIII. CONCLUSION

A numerical solution for the problem of electromagnetic transmission through an annular aperture in an infinite conducting screen of zero thickness is developed. The moment method is used to solve the integral equation for the equivalent magnetic current in the aperture. The expansion functions are subsectional in ρ and harmonic in ϕ. The number of subsections used is determined by the size of the aperture. The number of Fourier modes used can be determined, in general, from the size of the aperture, the angle of incidence and an inspection on the Bessel functions. The results are observed to converge with respect to the number of expansion functions and some of the results are compared with previous literature.

An attempt was made to use triangle expansion functions combined with the Fourier modes to solve the same problem, however, poorer results, especially for small apertures, were obtained. The edge condition of the ϕ-component of the magnetic current, and the fact that triangles are less independent from each other (they are actually 2-subsectional) than the pulses are suspected to be the cause of the failure.

Appendix A

FORMULAS FOR ELLIPTICALLY POLARIZED INCIDENCE

The general form of an elliptically polarized plane wave incidence can be written as:

$$\underline{E}^{io} = E_o(e_1 \hat{u}_{/\!/} + e_2 \hat{u}_{\perp})e^{-j\underline{k}\cdot\underline{r}} \tag{A-1}$$

where the normalization is done wuch that

$$|e_1|^2 + |e_2|^2 = 1 \tag{A-2}$$

The equivalent magnetic current for this incidence is simply the linear combination:

$$\underline{M}_o = E_o[(e_1 m_\rho^{/\!/} + e_2 m_\rho^{\perp})\underline{\hat{u}}_\rho + (e_1 m_\phi^{/\!/} + e_2 m_\phi^{\perp})\hat{u}_\phi] \tag{A-3}$$

where $m_\rho^{\perp}$, $m_\rho^{/\!/}$, $m_\phi^{\perp}$, $m_\phi^{/\!/}$ are defined in Sec. IV-b.

The far field components are linear quantities too:

$$F_\theta = E_o(e_1 f_\theta^{/\!/} + e_2 f_\theta^{\perp}) \tag{A-4}$$

$$F_\phi = E_o(e_1 f_\phi^{/\!/} + e_2 f_\phi^{\perp}) \tag{A-5}$$

where $f_\theta^{/\!/}$, $f_\theta^{\perp}$, $f_\phi^{/\!/}$, $f_\phi^{\perp}$ are defined in Sec. IV-b also.

The transmission coefficient is a power characteristic, but, since the cross products don't contribute (which can be seen from the symmetry), the total transmission is still a linear combination of those contributed by the two polarizations:

$$TC = \frac{\mathrm{Re}\left\{\sum_{n=o}^{N} \varepsilon_n \left(e_1 \begin{bmatrix} M\, \bar{v}_\rho^{n\parallel} \\ \\ \bar{v}_\phi^{n\parallel} \end{bmatrix}^{*T} \bar{i}^{n\parallel} + e_2 \begin{bmatrix} M\, \bar{v}_\rho^{n\perp} \\ \\ \bar{v}_\phi^{n\perp} \end{bmatrix}^{*T} \bar{i}^{n\perp}\right)\right\}}{M(M + 2x_o)/\eta_o} \qquad \text{(A-6)}$$

The normalized constants e_1 and e_2 for an elliptically polarized plane wave can be obtained from the ratio of the length of the minor axis to that of the major axis, r, the angle between the major axis and the vector $\hat{u}_{\parallel}$, ψ, where $0 \leq \psi \leq \pi$, and (when the wave is not linearly polarized) the helicity of the wave.

An elliptically polarized wave is said to be of positive (negative) helicity if the electric field vector rotates counterclockwise (clockwise) when the observer is facing into the oncoming wave.

If $r \neq 0$ and $r \neq 1$, e_1 and e_2 can be obtained as:

$$e_1 = r_1 \qquad \text{(A-7)}$$

$$e_2 = r_2\, e^{j\alpha} \qquad \text{(A-8)}$$

where

$$r_1 = \sqrt{\sin^2\psi + \frac{\cos 2\psi}{1 + r^2}} \qquad \text{(A-9)}$$

$$r_2 = \sqrt{\cos^2\psi - \frac{\cos 2\psi}{1 + r^2}} \qquad \text{(A-10)}$$

$$\alpha = \begin{cases} \cos^{-1}\left[\dfrac{\sin 2\psi(1 - r^2)}{2r_1 r_2\,(1 + r^2)}\right] - \pi & \text{for positive helicity} \\ \\ \cos^{-1}\left[\dfrac{\sin 2\psi(1 - r^2)}{2r_1 r_2\,(1 + r^2)}\right] & \text{for negative helcity} \end{cases} \qquad \text{(A-11)}$$

For the two special cases:

(i) When r = 1, the plane wave is circularly polarized and we have,

$$e_1 = \frac{1}{\sqrt{2}} \tag{A-12}$$

$$e_2 = \begin{cases} \dfrac{-j}{\sqrt{2}} & \text{for positive helicity} \\ \dfrac{j}{\sqrt{2}} & \text{for negative helcity} \end{cases} \tag{A-13}$$

(ii) When r = 0, the plane wave is linearly polarized and we have,

$$e_1 = \cos \psi \tag{A-14}$$

$$e_2 = \sin \psi \tag{A-15}$$

Appendix B

COMPUTER PROGRAM LISTING AND DESCRIPTION

Two programs are given in this section. One solves for the equivalent magnetic current and the other computes the power gain and transmission coefficient from this current. Section B-1.4 gives the description, listing and sample output of the first program. Sections B-1.1 to B-1.3 give the description and listing of the subprograms used. Section B-2.2 describes and lists the second program with its sample output. The subprogram used is given in B-2.1.

B-1.1. Subroutine CAD

Subroutine CAD(NP,N1,N2,RD,RI,LL,W,Q) computes submatrices $\approx{Y}^{N1}$, $\approx{Y}^{N1+1}$, ..., $\approx{Y}^{N2}$ of the admittance matrix. The constant factor $\frac{1}{\eta_o}$ is left out for all submatrices. Elements are stored in Y by columns and one submatrix after another, starting with the lowest mode ($\approx{Y}^{N1}$). The input variables are defined in terms of the variables introduced in previous sections as

NP = M, number of subdomains used.

RO = R_{out}, outer radius (in wavelengths) of the aperture.

RI = R_{in}, inner radius (in wavelengths) of the aperture.

LL = N_g , order of the Gaussian-quadrature integration in ϕ.

W(m) = w_m , weight factor of the Gaussian-quadrature integration in ϕ.

Q(m) = θ_m, abscissa of the Gaussian-quadrature integration in ϕ.

The output Y is transferred to the main program in the common block BLK2 by

```
COMMON /BLK2/Y
```

to avoid unnecessary storage space.

Minimum allocations are given by

```
COMPLEX Y(NY)
DIMENSION X(6), Q(LL), W(LL), SN(LL),
   CS(LL), U1(NL), U2(NL), U3(NL), D(NT),
   T(NT), R1(NT), R2(NT), R3(NT), R4(NT)
```

where

$$NY = (N2 - N1 + 1)(2M-1)^2$$

$$NL = (N2 - N1 + 1)LL$$

$$NT = 6\ LL$$

The matrix elements A^n_{pq}, B^n_{pq}, C^n_{pq} and D^n_{pq} are computed according to (80) to (83). The double DO loop 38 covers the ranges of both subscripts p,q. DO loop 36 does the Gaussian-quadrature integration in ϕ, or, equivalently, the summation $\sum_{m=1}^{N_g}$ in (80) to (83). DO loop 18 carries out the summation $\sum_{\ell=1}^{4}$ in (80) and (81). DO loops 14, 17, 23, 28, 32 and 35 cover the range n = N1, N1+1,...,N2 for all modes considered.

LISTING OF CAD

```
      SUBROUTINE CAD(NP,N1,N2,RO,RI,LL,W,Q)
      COMMON /BLK2/Y
      COMPLEX Y(2500),C,CJ,CR,CEXP,CE,E,F,G,H,AA,BB
      DIMENSION X(6),Q(30),SN(30),CS(30),U1(360),U2(360),U3(360), D(180)
     6,T(180),R1(180),R2(180),R3(180),R4(180),W(30)
      NR=NP-1
      NN=NR+NP
      NA=NN*NR
      NB=NA+NR
      NN2=NN**2
      JS=N1+1
      JF=N2+1
      JS1=JS+1
      JF1=JF+1
      JF2=JF+2
      JD=JF1-JS
      NT=NN2*JD
      PI=3.14159
      DD=RO-RI
      AK=(2*PI*DD)/NP
      CJ=(0.,1.)
      C=CJ*AK
      X0=(RI*NP)/DD
      DO 1 I=1,LL
      Q(I)=PI*(Q(I)+1)/2
      SN(I)=SIN(Q(I))
    1 CS(I)=COS(Q(I))
      K=0
      DO 2 I=1,LL
      DO 2 J=1,JD
      K=K+1
      U1(K)=0.
    2 U2(K)=0.
      DO 5 I=1,LL
      K=JD*(I-1)
      DO 5 J=JS,JF2
      K=K+1
      AC=COS((J-2)*Q(I))
      IF(J.GT.JF)GO TO 3
      U1(K)=U1(K)+AC/2.
      U2(K)=U2(K)-AC/2.
    3 IF(J.EQ.JS)GO TO 4
      IF(J.GT.JF1)GO TO 4
      K1=K-1
      U3(K1)=AC
    4 IF(J.LE.JS1)GO TO 5
      K2=K-2
      U1(K2)=U1(K2)+AC/2.
      U2(K2)=U2(K2)+AC/2.
    5 CONTINUE
      DO 6 I=1,4
    6 X(I)=X0+(I-2.5)/4.
      DO 7 I=1,NT
```

```
7       Y(I)=0.
        DO 38 I=1,NP
        DO 8 K=1,4
8       X(K)=X(K)+1.
        X(5)=X0+I-.5
        X(6)=X0+I+.5
        M=0
        DO 9 K=1,LL
        DO 9 L=1,6
        M=M+1
        T(M)=X0-X(L)*CS(K)
        D(M)=(X(L)*SN(K))**2
        R3(M)=SQRT(T(M)**2+D(M))
9       R4(M)=SQRT((T(M)+.5)**2+D(M))
        K2=NR+I
        K4=NB+I
        IF(I.EQ.NP)GO TO 10
        K1=I
        K3=NA+I
10      DO 38 J=1,NP
        M=0
        DO 11 K=1,LL
        DO 11 L=1,6
        M=M+1
        T(M)=T(M)+1.
        R1(M)=R3(M)
        R2(M)=R4(M)
        R3(M)=SQRT(T(M)**2+D(M))
11      R4(M)=SQRT((T(M)+.5)**2+D(M))
        K=0
        DO 36 M=1,LL
        JLL=JD*(M-1)
        IF(I.EQ.NP)GO TO 19
        DO 18 MP=1,4
        K=K+1
        TT=ABS(T(K)-.5)
        T1=TT+.5
        T2=TT-.5
        TA=T1+SQRT(T1**2+D(K))
        TB=T2+SQRT(T2**2+D(K))
        IF(T2.LT.0.)GO TO 12
        HT=ALOG(TA/TB)
        GO TO 13
12      TB=TB-2*T2
        HT=ALOG(TA*TB/D(K))
13      CR=C*R2(K)
        CE=CEXP(-CR)
        H=CE*((1+CR)*(R3(K)-R1(K)+X(MP)*CS(M)*HT)-C*(J-.5+X0))
        JLB=JLL
        JNB=K3
        AA=-AK*W(M)*H/4.
        DO 14 JN=JS,JF
        JLB=JLB+1
        Y(JNB)=Y(JNB)+AA*U2(JLB)
14      JNB=JNB+NN2
```

```
      IF(J.EQ.NP)GO TO 18
      SS=ABS(T(K))
      S1=SS+.5
      S2=SS-.5
      SA=S1+SQRT(S1**2+D(K))
      SB=S2+SQRT(S2**2+D(K))
      IF(S2.LT.0.)GO TO 15
      GT=ALOG(SA/SB)
      GO TO 16
15    SB=SB-2*S2
      GT=ALOG(SA*SB/D(K))
16    CR=C*R3(K)
      CE=CEXP(-CR)
      G=CE*((1.+CR)*GT-C)
      JLB=JLL
      JNB=K1
      AA=C*NP*W(M)*G/4.
      DO 17 JN=JS,JF
      JLB=JLB+1
      Y(JNB)=Y(JNB)+AA*U1(JLB)
17    JNB=JNB+NN2
18    CONTINUE
      GO TO 20
19    K=K+4
20    K=K+1
      TT=ABS(T(K)-.5)
      T1=TT+.5
      T2=TT-.5
      TA=T1+SQRT(T1**2+D(K))
      TB=T2+SQRT(T2**2+D(K))
      IF(T2.LT.0.)GO TO 21
      HT=ALOG(TA/TB)
      GO TO 22
21    TB=TB-2*T2
      HT=ALOG(TA*TB/D(K))
22    CR=C*R2(K)
      CE=CEXP(-CR)
      H=CE*((1+CR)*(R3(K)-R1(K)+X(5)*CS(M)*HT)-C*(J-.5+X0))
      G=CE*((1.+CR)*HT-C)
      JLB=JLL
      JNB=K4
      AA=C*W(M)*(I-.5+X0)*H
      BB=W(M)*G/C
      DO 23 JN=JS,JF
      JLB=JLB+1
      Y(JNB)=Y(JNB)+AA*U1(JLB)+(JN-1)**2*BB*U3(JLB)
23    JNB=JNB+NN2
      TT=ABS(T(K)+.5)
      T1=TT+.5
      T2=TT-.5
      TA=T1+SQRT(T1**2+D(K))
      TB=T2+SQRT(T2**2+D(K))
      IF(T2.LT.0.)GO TO 24
      GT=ALOG(TA/TB)
      GO TO 25
24    TB=TB-2*T2
```

```
      GT=ALOG(TA*TB/D(K))
25    CR=C*R4(K)
      CE=CEXP(-CR)
      E=CE*((1.+CR)*GT-C)
      IF(J.EQ.NP)GO TO 29
      SS=ABS(T(K))
      S1=SS+.5
      S2=SS-.5
      SA=S1+SQRT(S1**2+D(K))
      SB=S2+SQRT(S2**2+D(K))
      IF(S2.LT.0.)GO TO 26
      GT=ALOG(SA/SB)
      GO TO 27
26    SB=SB-S2*2
      GT=ALOG(SA*SB/D(K))
27    CR=C*R3(K)
      CE=CEXP(-CR)
      F=CE*((1.+CR)*GT-C)
      JLB=JLL
      JNB=K2
      AA=NP*W(M)*AK*(I-.5+X0)*F
      BB=-NP*W(M)*(G-E)/AK
      DO 28 JN=JS,JF
      JLB=JLB+1
      Y(JNB)=Y(JNB)+AA*U2(JLB)+(JN-1)*BB*U3(JLB)
28    JNB=JNB+NN2
29    K=K+1
      IF(I.EQ.NP)GO TO 36
      TT=ABS(T(K)-.5)
      T1=TT+.5
      T2=TT-.5
      TA=T1+SQRT(T1**2+D(K))
      TB=T2+SQRT(T2**2+D(K))
      IF(T2.LT.0.)GO TO 30
      HT=ALOG(TA/TB)
      GO TO 31
30    TB=TB-2*T2
      HT=ALOG(TA*TB/D(K))
31    CR=C*R2(K)
      CE=CEXP(-CR)
      F=CE*((1.+CR)*HT-C)
      JLB=JLL
      JNB=K3
      AA=-W(M)*(F-G)/AK
      DO 32 JN=JS,JF
      JLB=JLB+1
      Y(JNB)=Y(JNB)+(JN-1)*AA*U3(JLB)
32    JNB=JNB+NN2
      IF(J.EQ.NP)GO TO 36
      TT=ABS(T(K)+.5)
      T1=TT+.5
      T2=TT-.5
      TA=T1+SQRT(T1**2+D(K))
      TB=T2+SQRT(T2**2+D(K))
      IF(T2.LT.0.)GO TO 33
      GT=ALOG(TA/TB)
```

```
      GO TO 34
33    TB=TB-2*T2
      GT=ALOG(TA*TB/D(K))
34    CR=C*R4(K)
      CE=CEXP(-CR)
      H=CE*((1.+CR)*GT-C)
      JLB=JLL
      JNB=K1
      AA=-NP*W(M)*(F-G-H+E)/C
      DO 35 JN=JS,JF
      JLB=JLB+1
      Y(JNB)=Y(JNB)+AA*U3(JLB)
35    JNB=JNB+NN2
36    CONTINUE
      K4=K4+NN
      IF(I.EQ.NP)GO TO 37
      K3=K3+NN
37    IF(J.GE.NR)GO TO 38
      K2=K2+NN
      IF(I.EQ.NP)GO TO 38
      K1=K1+NN
38    CONTINUE
      RETURN
      END
```

B-1.2. Subroutine PEX

Subroutine PEX(AI,RO,RI,M,N) computes the column matrices $\bar{i}^{o\perp}$, $\bar{i}^{1\perp}$,..., $\bar{i}^{N\perp}$ for the $E_\perp$-polarization and $\bar{i}^{o/\!/}$, $\bar{i}^{1/\!/}$,...,$\bar{i}^{N/\!/}$ for the $E_{/\!/}$-polarization. The constant factor $\frac{1}{\eta_o}$ is left out for all matrices. The $\bar{i}^{n\perp}$'s are stored, starting from $\bar{i}^{o\perp}$, in W and $\bar{i}^{n/\!/}$'s in Q. The input variables are defined as

AI = θ^i , the angle of incidence, in degrees

RO = R_{out},the outer radius (in wavelengths) of the aperture.

RI = R_{in} ,the inner radius (in wavelengths) of the aperture.

M = M , number of subdomains used.

The outputs W and Q are transferred to the main program in the common block BLK1 by

Common /BLK1/W,Q

to avoid unnecessary storage space.

Minimum allocations are given by

```
COMPLEX W(NI), Q(NI)
DIMENSION X(M-1), Y(M)
COMMON  /BLK4/BJ(N+2)
```

where

NI = (2M-1)(N+1)

The matrix elements of $\bar{i}^{n\perp}$'s and $\bar{i}^{n/\!/}$'s are computed according to (106), (107), (124) and (125). DO loop 9 adds $J_n(x_q)$, n=0,1,...,N+1, q = 1,2,...,M-1, one at a time, to the proper elements of W,Q, with the proper constant factors. DO loop 14 has the same function for $J_n(x_{q-1/2})$'s.

If AI = 0 ($\theta^i = 0$), only $\bar{i}^{1\perp}$ and $\bar{i}^{1\parallel}$ are stored in W and Q and they are stored as W(2M) to W(4M-2) and Q(2M) to Q(4M-2). Simple computation are done without computing the Bessel functions. This is done by the control statement

```
IF(AI. EQ. 0.) GO TO 15
```

LISTING OF PEX

```
      SUBROUTINE PEX(AI,RO,RI,M,N)
      COMMON /BLK1/W,Q/BLK4/BJ(100)
      COMPLEX W(300),Q(300),CJ,CK,CA,TW,TQ
      DIMENSION X(24),Y(25)
      MM=M-1
      MD=M+MM
      NP=N+1
      NP2=NP+1
      MN=MD*NP
      D=RO-RI
      CJ=(0.,1.)
      X0=M*RI/D
      E=X0-.5
      DO 1 I=1,M
      E=E+1.
1     Y(I)=E
      E=X0
      DO 2 I=1,MM
      E=E+1.
2     X(I)=E
      IF(AI.EQ.0.)GO TO 15
      PI=3.141593
      A1=AI*PI/180.
      A=COS(A1)
      B=2.*PI*D*SIN(A1)/M
      CA=CJ*A
      DO 3 I=1,MN
      W(I)=0.
3     Q(I)=0.
      DO 9 I=1,MM
      T=B*X(I)
      CALL BES(NP,T)
      K=I
      IF(AI.EQ.90.)GO TO 4
      W(K)=-2.*CA*BJ(2)
4     CK=1.
      DO 9 J=1,NP2
      K=K+MD
      CK=CK/CJ
      IF(AI.EQ.90.)GO TO 5
      TW=CA*BJ(J)/CK
5     TQ=-BJ(J)/CK
      IF(J.GT.N)GO TO 7
      IF(AI.EQ.90.)GO TO 6
      W(K)=W(K)+TW
6     Q(K)=Q(K)-TQ
7     IF(J.LT.3)GO TO 9
      L=K-2*MD
      IF(AI.EQ.90.)GO TO 8
      W(L)=W(L)+TW
8     Q(L)=Q(L)+TQ
9     CONTINUE
```

```
      DO 14 I=1,M
      T=B*Y(I)
      CALL BES(NP,T)
      CK=1.
      K=I+MM
      Q(K)=-2.*CJ*Y(I)*BJ(2)
      DO 14 J=1,NP2
      K=K+MD
      CK=CK/CJ
      IF(AI.EQ.90.)GO TO 10
      TW=-A*Y(I)*BJ(J)/CK
10    TQ=CJ*Y(I)*BJ(J)/CK
      IF(J.GT.N)GO TO 12
      IF(AI.EQ.90.)GO TO 11
      W(K)=W(K)+TW
11    Q(K)=Q(K)+TQ
12    IF(J.LT.3)GO TO 14
      L=K-2*MD
      IF(AI.EQ.90.)GO TO 13
      W(L)=W(L)-TW
13    Q(L)=Q(L)+TQ
14    CONTINUE
      GO TO 18
15    K=MD
      DO 16 I=1,MM
      K=K+1
      Q(K)=-CJ
16    W(K)=1.
      DO 17 I=1,M
      K=K+1
      Q(K)=Y(I)
17    W(K)=CJ*Y(I)
18    RETURN
      END
```

B-1.3. Subroutines DECOMP, SOLVE and BES

The subroutines DECOMP and SOLVE uses the method of Gaussian elimination and LU decomposition to solve a linear system of equations with complex coefficients. These subroutines are described in [8]. Only input instructions and output descriptions are summarized here.

The input into DECOMP (N, IPS, UL) is N and the matrix $\tilde{\bar{A}}$ of coefficients of the set

$$\tilde{\bar{A}}\ \bar{x} = \bar{b}$$

of N linear equations stored by columns in UL. $N \geq 2$. The output from DECOMP is IPS and UL. DECOMP does not change N. SOLVE (N, IPS, UL, B, X) uses N, IPS, UL, and the elements of $\bar{b}$ stored in B to calculate and stored in X the elements of the solution $\bar{x}$. SOLVE does not change any of the input variables.

Minimum allocations are given by

```
COMPLEX UL(N²)
DIMENSION SCL(N), IPS(N)
```

in DECOMP and by

```
COMPLEX UL(N²), B(N), X(N)
DIMENSION IPS(N)
```

in SOLVE.

Subroutine BES(N,X) computes and store in BJ the values of $J_0(x)$, $J_1(x)$, ..., $J_N(x)$ by the numerical method in 9.12 on page 385 of [9].

Minimum allocation is given by

```
COMMON /BLK4/BJ(100)
```

LISTING OF DECOMP

```
      SUBROUTINE DECOMP(N,IPS,UL)
      COMPLEX UL(2500),PIVOT,EM
      DIMENSION SCL(50),IPS(50)
      DO 5 I=1,N
      IPS(I)=I
      RN=0.
      J1=I
      DO 2 J=1,N
      ULM=ABS(REAL(UL(J1)))+ABS(AIMAG(UL(J1)))
      J1=J1+N
      IF(RN-ULM) 1,2,2
1     RN=ULM
2     CONTINUE
      SCL(I)=1./RN
5     CONTINUE
      NM1=N-1
      K2=0
      DO 17 K=1,NM1
      BIG=0.
      DO 11 I=K,N
      IP=IPS(I)
      IPK=IP+K2
      SIZE=(ABS(REAL(UL(IPK)))+ABS(AIMAG(UL(IPK))))*SCL(IP)
      IF(SIZE-BIG) 11,11,10
10    BIG=SIZE
      IPV=I
11    CONTINUE
      IF(IPV-K) 14,15,14
14    J=IPS(K)
      IPS(K)=IPS(IPV)
      IPS(IPV)=J
15    KPP=IPS(K)+K2
      PIVOT=UL(KPP)
      KP1=K+1
      DO 16 I=KP1,N
      KP=KPP
      IP=IPS(I)+K2
      EM=-UL(IP)/PIVOT
18    UL(IP)=-EM
      DO 16 J=KP1,N
      IP=IP+N
      KP=KP+N
      UL(IP)=UL(IP)+EM*UL(KP)
16    CONTINUE
      K2=K2+N
17    CONTINUE
      RETURN
      END
```

LISTING OF SOLVE

```
      SUBROUTINE SOLVE(N,IPS,UL,B,X)
      COMPLEX UL(2500),B(50),X(50),SUM
      DIMENSION IPS(50)
      NP1=N+1
      IP=IPS(1)
      X(1)=B(IP)
      DO 2 I=2,N
      IP=IPS(I)
      IPB=IP
      IM1=I-1
      SUM=0.
      DO 1 J=1,IM1
      SUM=SUM+UL(IP)*X(J)
1     IP=IP+N
2     X(I)=B(IPB)-SUM
      K2=N*(N-1)
      IP=IPS(N)+K2
      X(N)=X(N)/UL(IP)
      DO 4 IBACK=2,N
      I=NP1-IBACK
      K2=K2-N
      IPI=IPS(I)+K2
      IP1=I+1
      SUM=0.
      IP=IPI
      DO 3 J=IP1,N
      IP=IP+N
3     SUM=SUM+UL(IP)*X(J)
4     X(I)=(X(I)-SUM)/UL(IPI)
      RETURN
      END
```

LISTING OF BES

```
      SUBROUTINE BES(N,X)
      COMMON /BLK4/BJ(100)/BLK3/Y0(33)
      PI=3.141593
      PI2=2./PI
      PI4=PI/4.
      PI7=.75*PI
      MZ=10+N+2*IFIX(X)
      BJ(MZ+1)=0.
      BJ(MZ)=1.E-60
      ALP=0.
      IF(MZ-(MZ/2)*2) 13,14,13
   14 JT=-1
      GO TO 15
   13 JT=1
   15 M2=MZ-2
```

```
      X2=2./X
      DO 16 K=1,M2
      MK=MZ-K
      BJ(MK)=X2*FLOAT(MK)*BJ(MK+1)-BJ(MK+2)
      JT=-JT
      S=1+JT
      ALP=ALP+BJ(MK)*S
   16 CONTINUE
      BJ(1)=X2*BJ(2)-BJ(3)
      ALP=ALP+BJ(1)
      NP=N+1
      DO 17 K=1,NP
      BJ(K)=BJ(K)/ALP
   17 CONTINUE
      RETURN
      END
```

B-1.4. Main Program 1.

This program treats an annular aperture with a number of incidences. For each incidence, the admittance matrix is the same, only excitations vary. Punched data cards are read early in the main program according to input statements in the following sequence.

```
101   FORMAT (I3)
102   FORMAT (2E14.7)
103   FORMAT (16F5.1)
104   FORMAT (26I3)
114   FORMAT (10F8.5)
      READ   (1,101)M
      READ   (1,101)ICASE
      READ   (1,101)LL
      READ   (1,102) RO,RI
      READ   (1,103) (AI(J), J=1, ICASE)
      READ   (1,104) (NS(J), J=1, ICASE)
      READ   (1,104) (NF(J), J=1, ICASE)
      READ   (1,114) (WW(J), J=1, LL)
      READ   (1,114) (QQ(J), J=1, LL)
```

The above input data is defined as

M = number of subdomains used.

ICASE = number of incidences considered.

LL = order of the Gaussian-quadrature integration in ϕ for admittance matrix elements.

RO,RI = outer and inner radius (in wavelengths) of the aperture, R_{out} and R_{in}.

AI(i) = angle of incidence of the ith incidence (in degrees).

NS(i) = order of the lowest mode used for the ith incidence.

NF(i) = order of the highest mode used for the ith incidence.

WW(i) = weight factor of the Gaussian-quadrature integration in ϕ.

QQ(i) = abscissa of the Gaussian-quadrature integration in ϕ.

Minimum allocations are given by

```
COMPLEX  Y(MY), Z(MZ), W(NI), Q(NI),
         P1(2M-1), P2(2M-1), V1(2M-1), V2(2M-1).
DIMENSION AI(ICASE), NS(ICASE), NF(ICASE)
         IPS(2M-1), IPSL(NI), WW(LL)
         QQ(LL)
```

where

$$MY = (\max (NF(i)) - \min (NS(i)) + 1)\ (2M-1)^2$$

$$MZ = (2M-1)^2$$

$$NI = (\max (NF(i)) + 1)\ (2M-1)$$

DO loop 3 determines the order of the highest and the lowest modes, MA and MI, needed for all incidences considered. These two integers are then fed into the subroutine CAD as the input parameters N1 and N2. In DO loop 6, admittance matrices $\tilde{\tilde{Y}}^{MI}$, $\tilde{\tilde{Y}}^{MI+1}$,..., $\tilde{\tilde{Y}}^{MA}$ are taken out of Y, one at a time, stored in Z, and fed into DECOMP, the output Z is stored back into Y and the output IPS is stored into IPSL for each mode. This is done early because the LU decomposition needs to be done only once for all excitations.

Different modes of different incidences are then treated in the double DO loop 14 where subroutine PEX is called to generate excitations for both polarizations according to the modes specified for each incidence. Different modes are then solved for each incidence. Here, submatrices for each mode are again taken out of Y and IPSL and fed into SOLVE together with the proper excitation matrices. The output V1 is the solution $\bar{v}^{n\perp}$ and the output V2 is the solution $\bar{v}^{n\parallel}$.

Notice that the current solutions are printed out at each stage but not kept in a permanent storage. Data should be punched out, if needed, inside the DO loops.

PROGRAM 1

```
      COMMON /BLK1/W,Q/BLK2/Y/BLK3/Y0(33)
      COMPLEX Y(2500),Z(2500),W(300),Q(300),P1(50),P2(50),V1(50),V2(50),
     6CJ,VT
      DIMENSION AI(20),NS(20),NF(20),IPS(50),IPSL(300),WW(30),QQ(30)
101   FORMAT(I3)
102   FORMAT(2E14.7)
103   FORMAT(16F5.1)
104   FORMAT(26I3)
105   FORMAT('1',1X,'ANNULAR APERTURE PROBLEM',///)
106   FORMAT(5X,'OUTER RADIUS/WAVELENGTH',4X,'INNER RADIUS/WAVELENGTH',4
     6X,'NUMBER OF SUBDOMAINS',/,11X,E12.5,16X,E12.5,17X,I2,//)
107   FORMAT(5X,'CASE',3X,'ANGLE OF INCIDENCE',3X,'MODES USED',/,16X,'(D
     6EGREES)',//)
108   FORMAT(5X,I3,10X,F5.1,10X,I3,' TO',I2)
109   FORMAT('1',5X,'EQUIVALENT MAGNETIC CURRENT:',///)
110   FORMAT(6X,'CASE',I3,//)
111   FORMAT(/,7X,'N=',I2,//,11X,'VERTICAL POLARIZATION',/)
112   FORMAT(11X,I2,5E12.4)
113   FORMAT(11X,I2,2X,'0.',10X,'0.',10X,'0.')
114   FORMAT(10F8.5)
115   FORMAT(/,11X,'HORIZONTAL POLARIZATION',/)
116   FORMAT(////,5X,I3,' POINTS GAUSSIAN QUADRATURE INTEGRATION IS USED
     6')
      READ(1,101)M
      READ(1,101)ICASE
      READ(1,101)LL
      READ(1,102)RO,RI
      READ(1,103)(AI(J),J=1,ICASE)
      READ(1,104)(NS(J),J=1,ICASE)
      READ(1,104)(NF(J),J=1,ICASE)
      READ(1,114)(WW(J),J=1,LL)
      READ(1,114)(QQ(J),J=1,LL)
      WRITE(3,105)
      WRITE(3,106)RO,RI,M
      WRITE(3,107)
      MM=M-1
      MD=M+MM
      MD2=MD**2
      CJ=(0.,1.)
      X0=M*RI/(RO-RI)
      DO 1 J=1,ICASE
1     WRITE(3,108)J,AI(J),NS(J),NF(J)
      WRITE(3,116)LL
      MA=0
      MI=100000
      DO 3 J=1,ICASE
      IF(NS(J).GE.MI)GO TO 2
      MI=NS(J)
2     IF(NF(J).LE.MA)GO TO 3
      MA=NF(J)
3     CONTINUE
      CALL CAD(M,MI,MA,RO,RI,LL,WW,QQ)
      K=0
```

```
      KK=0
      L=0
      ND=MA-MI+1
      DO 6 J=1,ND
      DO 4 N=1,MD2
      K=K+1
4     Z(N)=Y(K)
      CALL DECOMP(MD,IPS,Z)
      DO 5 N=1,MD2
      KK=KK+1
5     Y(KK)=Z(N)
      DO 6 N=1,MD
      L=L+1
6     IPSL(L)=IPS(N)
      WRITE(3,109)
      DO 14 J=1,ICASE
      WRITE(3,110)J
      JS=NS(J)
      JS1=JS+1
      JF=NF(J)
      JF1=JF+1
      AN=AI(J)
      CALL PEX(AN,RO,RI,M,JF)
      K=MD2*(JS-MI)
      L=MD*JS
      LL=MD*(JS-MI)
      DO 14 N=JS1,JF1
      N1=N-1
      DO 7 I=1,MD2
      K=K+1
7     Z(I)=Y(K)
      DO 8 I=1,MD
      L=L+1
      LL=LL+1
      P1(I)=W(L)
      P2(I)=Q(L)
8     IPS(I)=IPSL(LL)
      CALL SOLVE(MD,IPS,Z,P1,V1)
      CALL SOLVE(MD,IPS,Z,P2,V2)
      WRITE(3,111)N1
      DO 9 I=1,MM
      VT=V1(I)*M/(X0+I)
      VTA=CABS(VT)
      IF(N1.EQ.0)GO TO 9
      VT=VT*2
      VTA=VTA*2
9     WRITE(3,112)I,V1(I),VT,VTA
      DO 11 I=1,M
      IF(N1.EQ.0)GO TO 10
      II=I+MM
      VT=2*CJ*V1(II)
      VTA=CABS(VT)
      WRITE(3,112)I,V1(II),VT,VTA
      GO TO 11
10    WRITE(3,113)I
```

```
11      CONTINUE
        WRITE(3,115)
        DO 13 I=1,MM
        IF(N1.EQ.0)GO TO 12
        VT=2*CJ*V2(I)*M/(X0+I)
        VTA=CABS(VT)
        WRITE(3,112)I,V2(I),VT,VTA
        GO TO 13
12      WRITE(3,113)I
13      CONTINUE
        DO 14 I=1,M
        II=I+MM
        VT=V2(II)
        VTA=CABS(VT)
        IF(N1.EQ.0)GO TO 14
        VT=VT*2
        VTA=VTA*2
14      WRITE(3,112)I,V2(II),VT,VTA
        STOP
        END
```

SAMPLE OUTPUT

```
OUTER RADIUS/WAVELENGTH     INNER RADIUS/WAVELENGTH     NUMBER OF SUBDOMAINS
      0.20000E-01                   0.00000E 00                   15

CASE   ANGLE OF INCIDENCE   MODES USED
           (DEGREES)

  1           0.0              1 TO 1
  2          30.0              0 TO 1


 20 POINTS GAUSSIAN QUADRATURE INTEGRATION IS USED
```

EQUIVALENT MAGNETIC CURRENT:

CASE 1

N= 1

VERTICAL POLARIZATION

1	0.1586E-05	0.3686E-02	0.4758E-04	0.1106E 00	0.1106E 00
2	0.2885E-05	0.6966E-02	0.4328E-04	0.1045E 00	0.1045E 00
3	0.4292E-05	0.1043E-01	0.4292E-04	0.1043E 00	0.1043E 00
4	0.5626E-05	0.1366E-01	0.4219E-04	0.1025E 00	0.1025E 00
5	0.6880E-05	0.1671E-01	0.4128E-04	0.1003E 00	0.1003E 00
6	0.8061E-05	0.1949E-01	0.4031E-04	0.9743E-01	0.9743E-01
7	0.9075E-05	0.2195E-01	0.3889E-04	0.9406E-01	0.9406E-01
8	0.9901E-05	0.2398E-01	0.3713E-04	0.8993E-01	0.8993E-01
9	0.1053E-04	0.2550E-01	0.3509E-04	0.8501E-01	0.8501E-01
10	0.1090E-04	0.2637E-01	0.3270E-04	0.7912E-01	0.7912E-01
11	0.1092E-04	0.2641E-01	0.2977E-04	0.7203E-01	0.7203E-01
12	0.1047E-04	0.2536E-01	0.2617E-04	0.6339E-01	0.6339E-01
13	0.9382E-05	0.2269E-01	0.2165E-04	0.5236E-01	0.5236E-01
14	0.7366E-05	0.1786E-01	0.1578E-04	0.3827E-01	0.3827E-01
1	-0.5538E-01	0.2382E-04	-0.4764E-04	-0.1108E 00	0.1108E 00
2	-0.4998E-01	0.1991E-04	-0.3982E-04	-0.9996E-01	0.9996E-01
3	-0.5427E-01	0.2233E-04	-0.4465E-04	-0.1085E 00	0.1085E 00
4	-0.5292E-01	0.2248E-04	-0.4496E-04	-0.1058E 00	0.1058E 00
5	-0.5337E-01	0.2299E-04	-0.4598E-04	-0.1067E 00	0.1067E 00
6	-0.5329E-01	0.2415E-04	-0.4831E-04	-0.1066E 00	0.1066E 00
7	-0.5379E-01	0.2450E-04	-0.4901E-04	-0.1076E 00	0.1076E 00
8	-0.5396E-01	0.2530E-04	-0.5061E-04	-0.1079E 00	0.1079E 00
9	-0.5447E-01	0.2684E-04	-0.5368E-04	-0.1089E 00	0.1089E 00
10	-0.5529E-01	0.2888E-04	-0.5777E-04	-0.1106E 00	0.1106E 00
11	-0.5659E-01	0.3111E-04	-0.6222E-04	-0.1132E 00	0.1132E 00
12	-0.5901E-01	0.3459E-04	-0.6917E-04	-0.1180E 00	0.1180E 00
13	-0.6393E-01	0.4099E-04	-0.8198E-04	-0.1279E 00	0.1279E 00
14	-0.7049E-01	0.4856E-04	-0.9712E-04	-0.1410E 00	0.1410E 00
15	-0.1507E 00	0.1203E-03	-0.2407E-03	-0.3013E 00	0.3013E 00

HORIZONTAL POLARIZATION

1	0.3686E-02	-0.1586E-05	0.4758E-04	0.1106E 00	0.1106E 00
2	0.6966E-02	-0.2885E-05	0.4328E-04	0.1045E 00	0.1045E 00
3	0.1043E-01	-0.4292E-05	0.4292E-04	0.1043E 00	0.1043E 00
4	0.1366E-01	-0.5626E-05	0.4219E-04	0.1025E 00	0.1025E 00
5	0.1671E-01	-0.6880E-05	0.4128E-04	0.1003E 00	0.1003E 00
6	0.1949E-01	-0.8061E-05	0.4031E-04	0.9743E-01	0.9743E-01
7	0.2195E-01	-0.9075E-05	0.3889E-04	0.9406E-01	0.9406E-01
8	0.2398E-01	-0.9901E-05	0.3713E-04	0.8993E-01	0.8993E-01
9	0.2550E-01	-0.1053E-04	0.3509E-04	0.8501E-01	0.8501E-01
10	0.2637E-01	-0.1090E-04	0.3270E-04	0.7912E-01	0.7912E-01
11	0.2641E-01	-0.1092E-04	0.2977E-04	0.7203E-01	0.7203E-01
12	0.2536E-01	-0.1047E-04	0.2617E-04	0.6339E-01	0.6339E-01
13	0.2269E-01	-0.9382E-05	0.2165E-04	0.5236E-01	0.5236E-01
14	0.1786E-01	-0.7366E-05	0.1578E-04	0.3827E-01	0.3827E-01

1	0.2382E-04	0.5538E-01	0.4764E-04	0.1108E 00	0.1108E 00
2	0.1991E-04	0.4998E-01	0.3982E-04	0.9996E-01	0.9996E-01
3	0.2233E-04	0.5427E-01	0.4465E-04	0.1085E 00	0.1085E 00
4	0.2248E-04	0.5292E-01	0.4496E-04	0.1058E 00	0.1058E 00
5	0.2299E-04	0.5337E-01	0.4598E-04	0.1067E 00	0.1067E 00
6	0.2415E-04	0.5329E-01	0.4831E-04	0.1066E 00	0.1066E 00
7	0.2450E-04	0.5379E-01	0.4901E-04	0.1076E 00	0.1076E 00
8	0.2530E-04	0.5396E-01	0.5061E-04	0.1079E 00	0.1079E 00
9	0.2684E-04	0.5447E-01	0.5368E-04	0.1089E 00	0.1089E 00
10	0.2888E-04	0.5529E-01	0.5777E-04	0.1106E 00	0.1106E 00
11	0.3111E-04	0.5659E-01	0.6222E-04	0.1132E 00	0.1132E 00
12	0.3459E-04	0.5901E-01	0.6917E-04	0.1180E 00	0.1180E 00
13	0.4099E-04	0.6393E-01	0.8198E-04	0.1279E 00	0.1279E 00
14	0.4856E-04	0.7049E-01	0.9712E-04	0.1410E 00	0.1410E 00
15	0.1203E-03	0.1507E 00	0.2407E-03	0.3013E 00	0.3013E 00

CASE 2

N= 0

VERTICAL POLARIZATION

1	0.5245E-05	0.3556E-12	0.7868E-04	0.5334E-11	0.7868E-04
2	0.2426E-04	0.1975E-11	0.1819E-03	0.1481E-10	0.1819E-03
3	0.5530E-04	-0.4101E-13	0.2765E-03	-0.2051E-12	0.2765E-03
4	0.9759E-04	0.1070E-12	0.3660E-03	0.4014E-12	0.3660E-03
5	0.1498E-03	-0.2058E-11	0.4494E-03	-0.6173E-11	0.4494E-03
6	0.2102E-03	-0.1431E-10	0.5256E-03	-0.3576E-10	0.5256E-03
7	0.2765E-03	-0.1430E-10	0.5926E-03	-0.3063E-10	0.5926E-03
8	0.3457E-03	-0.2783E-10	0.6482E-03	-0.5217E-10	0.6482E-03
9	0.4139E-03	-0.3645E-10	0.6899E-03	-0.6074E-10	0.6899E-03
10	0.4760E-03	-0.4206E-10	0.7140E-03	-0.6308E-10	0.7140E-03
11	0.5249E-03	-0.6040E-10	0.7158E-03	-0.8236E-10	0.7158E-03
12	0.5504E-03	-0.5965E-10	0.6880E-03	-0.7456E-10	0.6880E-03
13	0.5341E-03	-0.6078E-10	0.6163E-03	-0.7013E-10	0.6163E-03
14	0.4558E-03	-0.5202E-10	0.4883E-03	-0.5574E-10	0.4883E-03

1	0.	0.
2	0.	0.
3	0.	0.
4	0.	0.
5	0.	0.
6	0.	0.
7	0.	0.
8	0.	0.
9	0.	0.
10	0.	0.
11	0.	0.
12	0.	0.
13	0.	0.
14	0.	0.
15	0.	0.

HORIZONTAL POLARIZATION

1	0.	0.
2	0.	0.
3	0.	0.
4	0.	0.
5	0.	0.
6	0.	0.
7	0.	0.
8	0.	0.
9	0.	0.
10	0.	0.
11	0.	0.
12	0.	0.
13	0.	0.
14	0.	0.

1	-0.1113E-01	-0.5055E-05	-0.1113E-01	-0.5055E-05	0.1113E-01
2	-0.3172E-01	-0.9362E-05	-0.3172E-01	-0.9362E-05	0.3172E-01
3	-0.5352E-01	-0.1493E-04	-0.5352E-01	-0.1493E-04	0.5352E-01
4	-0.7611E-01	-0.2101E-04	-0.7611E-01	-0.2101E-04	0.7611E-01
5	-0.9989E-01	-0.2740E-04	-0.9989E-01	-0.2740E-04	0.9989E-01
6	-0.1254E 00	-0.3436E-04	-0.1254E 00	-0.3436E-04	0.1254E 00
7	-0.1531E 00	-0.4188E-04	-0.1531E 00	-0.4188E-04	0.1531E 00
8	-0.1842E 00	-0.5064E-04	-0.1842E 00	-0.5064E-04	0.1842E 00
9	-0.2197E 00	-0.6003E-04	-0.2197E 00	-0.6003E-04	0.2197E 00
10	-0.2620E 00	-0.7187E-04	-0.2620E 00	-0.7187E-04	0.2620E 00
11	-0.3146E 00	-0.8596E-04	-0.3146E 00	-0.8596E-04	0.3146E 00
12	-0.3842E 00	-0.1050E-03	-0.3842E 00	-0.1050E-03	0.3842E 00
13	-0.4906E 00	-0.1342E-03	-0.4906E 00	-0.1342E-03	0.4906E 00
14	-0.6276E 00	-0.1713E-03	-0.6276E 00	-0.1713E-03	0.6276E 00
15	-0.1700E 01	-0.4639E-03	-0.1700E 01	-0.4639E-03	0.1700E 01

N= 1

VERTICAL POLARIZATION

1	-0.1393E-05	-0.3148E-02	-0.4178E-04	-0.9445E-01	0.9445E-01
2	-0.2488E-05	-0.6069E-02	-0.3732E-04	-0.9104E-01	0.9104E-01
3	-0.3726E-05	-0.9077E-02	-0.3726E-04	-0.9077E-01	0.9077E-01
4	-0.4873E-05	-0.1184E-01	-0.3655E-04	-0.8881E-01	0.8881E-01
5	-0.5957E-05	-0.1448E-01	-0.3574E-04	-0.8687E-01	0.8687E-01
6	-0.6980E-05	-0.1688E-01	-0.3490E-04	-0.8438E-01	0.8438E-01
7	-0.7857E-05	-0.1900E-01	-0.3367E-04	-0.8144E-01	0.8144E-01
8	-0.8572E-05	-0.2076E-01	-0.3214E-04	-0.7786E-01	0.7786E-01
9	-0.9113E-05	-0.2208E-01	-0.3038E-04	-0.7360E-01	0.7360E-01
10	-0.9437E-05	-0.2283E-01	-0.2831E-04	-0.6849E-01	0.6849E-01
11	-0.9451E-05	-0.2286E-01	-0.2577E-04	-0.6235E-01	0.6235E-01
12	-0.9064E-05	-0.2194E-01	-0.2266E-04	-0.5486E-01	0.5486E-01
13	-0.8122E-05	-0.1964E-01	-0.1874E-04	-0.4531E-01	0.4531E-01
14	-0.6376E-05	-0.1546E-01	-0.1366E-04	-0.3312E-01	0.3312E-01

1	0.4730E-01	-0.2092E-04	0.4184E-04	0.9459E-01	0.9459E-01
2	0.4449E-01	-0.1679E-04	0.3359E-04	0.8899E-01	0.8899E-01
3	0.4707E-01	-0.1963E-04	0.3926E-04	0.9414E-01	0.9414E-01
4	0.4536E-01	-0.1934E-04	0.3869E-04	0.9072E-01	0.9072E-01
5	0.4615E-01	-0.1988E-04	0.3977E-04	0.9230E-01	0.9230E-01
6	0.4608E-01	-0.2090E-04	0.4180E-04	0.9215E-01	0.9215E-01
7	0.4655E-01	-0.2121E-04	0.4243E-04	0.9309E-01	0.9309E-01
8	0.4669E-01	-0.2190E-04	0.4380E-04	0.9339E-01	0.9339E-01
9	0.4718E-01	-0.2323E-04	0.4646E-04	0.9435E-01	0.9435E-01
10	0.4780E-01	-0.2501E-04	0.5002E-04	0.9560E-01	0.9560E-01
11	0.4900E-01	-0.2693E-04	0.5386E-04	0.9800E-01	0.9800E-01
12	0.5106E-01	-0.2994E-04	0.5988E-04	0.1021E 00	0.1021E 00
13	0.5536E-01	-0.3548E-04	0.7097E-04	0.1107E 00	0.1107E 00
14	0.6102E-01	-0.4203E-04	0.8407E-04	0.1220E 00	0.1220E 00
15	0.1304E 00	-0.1042E-03	0.2084E-03	0.2608E 00	0.2608E 00

HORIZONTAL POLARIZATION

1	-0.3182E-02	0.1589E-05	-0.4768E-04	-0.9546E-01	0.9546E-01
2	-0.6073E-02	0.2880E-05	-0.4320E-04	-0.9109E-01	0.9109E-01
3	-0.9157E-02	0.4293E-05	-0.4293E-04	-0.9157E-01	0.9157E-01
4	-0.1196E-01	0.5604E-05	-0.4203E-04	-0.8971E-01	0.8971E-01
5	-0.1463E-01	0.6871E-05	-0.4123E-04	-0.8778E-01	0.8778E-01
6	-0.1705E-01	0.8056E-05	-0.4028E-04	-0.8527E-01	0.8527E-01
7	-0.1921E-01	0.9061E-05	-0.3883E-04	-0.8231E-01	0.8231E-01
8	-0.2099E-01	0.9886E-05	-0.3707E-04	-0.7870E-01	0.7870E-01
9	-0.2232E-01	0.1051E-04	-0.3504E-04	-0.7439E-01	0.7439E-01
10	-0.2307E-01	0.1089E-04	-0.3266E-04	-0.6922E-01	0.6922E-01
11	-0.2311E-01	0.1090E-04	-0.2973E-04	-0.6303E-01	0.6303E-01
12	-0.2218E-01	0.1046E-04	-0.2615E-04	-0.5545E-01	0.5545E-01
13	-0.1985E-01	0.9369E-05	-0.2162E-04	-0.4580E-01	0.4580E-01
14	-0.1561E-01	0.7359E-05	-0.1577E-04	-0.3346E-01	0.3346E-01
1	-0.2388E-04	-0.4782E-01	-0.4775E-04	-0.9563E-01	0.9563E-01
2	-0.1978E-04	-0.4414E-01	-0.3956E-04	-0.8829E-01	0.8829E-01
3	-0.2243E-04	-0.4851E-01	-0.4486E-04	-0.9703E-01	0.9703E-01
4	-0.2212E-04	-0.4655E-01	-0.4424E-04	-0.9310E-01	0.9310E-01
5	-0.2319E-04	-0.4764E-01	-0.4638E-04	-0.9527E-01	0.9527E-01
6	-0.2420E-04	-0.4803E-01	-0.4839E-04	-0.9606E-01	0.9606E-01
7	-0.2438E-04	-0.4917E-01	-0.4875E-04	-0.9833E-01	0.9833E-01
8	-0.2526E-04	-0.5012E-01	-0.5053E-04	-0.1002E 00	0.1002E 00
9	-0.2684E-04	-0.5161E-01	-0.5368E-04	-0.1032E 00	0.1032E 00
10	-0.2886E-04	-0.5353E-01	-0.5772E-04	-0.1071E 00	0.1071E 00
11	-0.3106E-04	-0.5649E-01	-0.6212E-04	-0.1130E 00	0.1130E 00
12	-0.3464E-04	-0.6088E-01	-0.6929E-04	-0.1218E 00	0.1218E 00
13	-0.4092E-04	-0.6887E-01	-0.8184E-04	-0.1377E 00	0.1377E 00
14	-0.4859E-04	-0.7931E-01	-0.9718E-04	-0.1586E 00	0.1586E 00
15	-0.1203E-03	-0.1841E 00	-0.2405E-03	-0.3682E 00	0.3682E 00

Data for equivalent magnetic current in the above sample output is arranged as follows. The first and second columns are the real and imaginary parts of the elements of $\bar{v}^{n\perp}$ and $\bar{v}^{n\parallel}$ for the two polarizations. For the $E_\perp$-polarization, the last three columns are the real part, the imaginary part and the magnitude of $\frac{\varepsilon_n M v_{\rho q}^{n\perp}}{(x_o+q)}$ and $\varepsilon_n j\, v_{\phi q}^{n\perp}$. For the E - polarization, the last three columns are the real part, the imaginary part and the magnitude of $\frac{\varepsilon_n j M v_{\rho q}^{n\parallel}}{(x_o+q)}$ and $\varepsilon_n v_{\phi q}^{n\parallel}$. The significance of these last three columns is obvious from (117) to (119) and (132) to (134). Notice that $\bar{v}_\phi^{o\perp}$ and $\bar{v}_\rho^{o\parallel}$ are always zero matrices and only the first two columns are printed for them.

B-2.1. Subroutine FAR

Subroutine FAR (THETA, PE, PH, PEC, PHC, TC) computes the following two quantities: (1) the integral

$$t(\theta) = \frac{r^2 \sin\theta}{P_{in}} \int_0^{2\pi} \frac{k^2}{2\eta_o} (|F_\phi|^2 + |F_\theta|^2) d\phi \tag{B-1}$$

and (2) the ratio

$$G'(\theta,\phi) = \Pi r^2 \frac{k^2}{\eta_o} (|F_\phi|^2 + |F_\theta|^2)/P_{in} \tag{B-2}$$

Notice that the transmission coefficient and the power gain can be related to the above quantities by

$$TC = \int_0^{\pi/2} t(\theta) d\theta \tag{B-3}$$

and

$$G(\theta,\phi) = G'(\theta,\phi)/TC \tag{B-4}$$

F_θ, F_ϕ are computed according to (147) to (150) and (151) to (154). The integration in (B-1) is carried out analytically by integrating the trigonometric functions.

This subroutine treats a number of indicences at the same time. $t(\theta)$ for each incidence is computed and stored in TC. $G'(\theta,\phi)$ for each incidence is computed in two different planes. If ϕ_1 and ϕ_2 specify the two planes for the ith incidence, then, $G'(\theta,\phi_1)$, $G'(\theta,\phi_2)$, $G'(\theta,\phi_1+\pi)$ and $G'(\theta,\phi_2+\pi)$ are stored as the ith element of arrays PE, PH, PEC and PHC respectively. The input variables are defined as

THETA = θ, the elevation angle (in radians)

X(i) = x_i, Y(i) = $x_{i-1/2}$ as defined by (92)

IMS(i) = the order of the lowest mode used for the ith incidence

IMF(i) = the order of the highest mode used for the ith incidence

PHE(i) = angle specifying the first plane for pattern of the ith incidence (in degrees).

PHH(i) = angle specifying the second plane for pattern of the ith incidence (in degrees).

W stores the $e_2\bar{v}^{n\perp}$'s starting with the lowest mode of the first incidence.

Q stores the $e_1\bar{v}^{n/\!/}$'s starting with the lowest mode of the first incidence.

ICASE = the number of incidences considered.

NMAX = the order of the highest mode used for all incidences considered.

M = number of subdomains used.

AK = κ as defined by (84).

RI = R_{in} inner radius (in wavelengths) of the aperture.

Minimum allocations are given by

```
COMPLEX W(NW), Q(NW), CFP(NI), CFT(NI)
DIMENSION PE(ICASE), PH(ICASE), PEC(ICASE),
          PHC(ICASE),TC(ICASE)
COMMON    /BKF1/X(M-1), Y(M), IMS(ICASE),
          IMF(ICASE), PHE(ICASE), PHH(ICASE)
          /BKF4/BJ(NB)
```

where $$NW = (2M-1) \sum_{q=1}^{ICASE} [IMF(q) - IMS(q) + 1]$$

$$NI = (2M-1)\ NMAX$$

$$NB = NMAX + 3$$

DO loops 2 and 3 compute and store in CFP and CFT the coefficients of $v_{\rho q}^{n}$'s and $v_{\phi q}^{n}$'s as in (149) and (150). These two arrays are defined as

$$\overline{CFP} = \begin{bmatrix} \overline{CFP}^{0} \\ \overline{CFP}^{1} \\ \vdots \\ \overline{CFP}^{NMAX} \end{bmatrix} \tag{B-5}$$

$$\overline{CFT} = \begin{bmatrix} \overline{CFT}^{0} \\ \overline{CFT}^{1} \\ \vdots \\ \overline{CFT}^{NMAX} \end{bmatrix} \tag{B-6}$$

where

$$CFP^{n}(\ell) = \begin{cases} j^{n+1} M[J_{n+1}(\kappa x_{\ell} \sin\theta) + J_{n-1}(\kappa x_{\ell} \sin\theta)] \\ \qquad \text{for } \ell = 1,2,\ldots,M-1 \\ -\, j^{n}\{x_{\ell-M+1/2}[J_{n+1}(\kappa x_{\ell-M+1/2} \sin\theta) - J_{n-1}(\kappa x_{\ell-M+1/2} \sin\theta)] \\ +\, \frac{\kappa \sin\theta}{24}\,[2J_{n}(\kappa x_{\ell-M+1/2} \sin\theta) - J_{n+2}(\kappa x_{\ell-M+1/2} \sin\theta) \\ \qquad -\, J_{n-2}(\kappa x_{\ell-M+1/2} \sin\theta)]\} \\ \qquad \text{for } \ell = M,\ldots,2M-1 \end{cases} \tag{B-7}$$

$$\mathrm{CFT}^n(\ell) = \begin{cases} j^{n+1} M\,[J_{n+1}(\kappa x_\ell \sin\theta) - J_{n-1}(\kappa x_\ell \sin\theta)] \\ \qquad\qquad\qquad \text{for } \ell = 1,2,\ldots,M-1 \\ -j^n\{x_{\ell-M+1/2}[J_{n+1}(\kappa x_{\ell-M+1/2}\sin\theta) + J_{n-1}(\kappa x_{\ell-M+1/2}\sin\theta)] \\ -\dfrac{\kappa \sin\theta}{24}\,[J_{n+2}(\kappa x_{\ell-M+1/2}\sin\theta) - J_{n-2}(\kappa x_{\ell-M+1/2}\sin\theta)]\} \\ \qquad\qquad\qquad \text{for } \ell = M,\ldots,2M-1 \end{cases} \tag{B-8}$$

DO loops 5, 6 and 7 compute, for the ith incidence, $f(\theta)$ and $G'(\theta-\phi)$, according to the formulas

$$t(\theta) = \frac{\kappa^2 \sin\theta}{M(M+2x_o)} \sum_{n=\mathrm{IMS}(i)}^{\mathrm{IMF}(i)} \{\frac{\varepsilon_n}{2}\,|\overline{\mathrm{CFP}^n}^T e_1 \bar{v}^{n\parallel}|^2 + \cos^2\theta\,|\overline{\mathrm{CFT}^n}^T e_1 \bar{v}^{n\parallel}|^2 + \frac{\varepsilon_n}{2}\cos^2\theta\,|\overline{\mathrm{CFT}^n}^T e_2 \bar{v}^{n\perp}|^2 + |\overline{\mathrm{CFP}^n}^T e_2 \bar{v}^{n\perp}|^2\} \tag{B-9}$$

and

$$G'(\theta,\phi) = \frac{2\kappa^2}{M(M+2x_o)}\{|\sum_{n=\mathrm{IMS}(i)}^{\mathrm{IMF}(i)} [\frac{\varepsilon_n}{2}\cos n\phi\, e_1 \bar{v}^{n\parallel} + \sin n\phi\, e_2 \bar{v}^{n\perp}]^T\, \overline{\mathrm{CFP}^n}|^2 + \cos^2\theta\,|\sum_{n=\mathrm{IMS}(i)}^{\mathrm{IMF}(i)} [\sin n\phi\, e_1 \bar{v}^{n\parallel} + \frac{\varepsilon_n}{2}\cos n\phi\, e_2 \bar{v}^{n\perp}]^T\, \overline{\mathrm{CFT}^n}|^2\} \tag{B-10}$$

Subroutine BES, as introduced in B-1.3 is called in this subroutine. Notice this time, the output BJ of BES is transferred in the common block BLKF4.

LISTING OF FAR

```
      SUBROUTINE FAR(THETA,PE,PH,PEC,PHC,TC)
      COMMON /BLKF1/X(50),Y(50),IMS(20),IMF(20),PHE(20),PHH(20)/BLKF2/W,
     6Q/BLKF3/ICASE,NMAX,M,AK,RI/BLKF4/BJ(100)
      COMPLEX W(2000),Q(2000),CFP(250),CFT(250),CJ,CK,FTE,FTH,FPE,FPH,SP
     6W,SPQ,STW,STQ,FPEC,FPHC,FTEC,FTHC,TERM
      DIMENSION PE(20),PH(20),TC(20),PEC(20),PHC(20)
      PI=3.141593
      CJ=(0.,1.)
      MM=M-1
      MD=M+MM
      X0=2*PI*RI/AK
      AK2=AK**2
      AREA=M*(M+2*X0)/AK2
      B=AK*SIN(THETA)
      N1=NMAX+1
      N2=N1+1
      N3=N2+1
      BS=B/24
      BC=COS(THETA)
      DO 2 I=1,MM
      T=B*X(I)
      CALL BES(N1,T)
      DO 1 J=1,N2
    1 BJ(J)=M*BJ(J)
      CFT(I)=2*CJ*BJ(2)
      CFP(I)=0.
      K=I
      CK=1.
      L1=2
      L2=0
      DO 2 J=1,NMAX
      K=K+MD
      L1=L1+1
      L2=L2+1
      CK=CK*CJ
      CFP(K)=CK*(BJ(L1)+BJ(L2))
    2 CFT(K)=CJ*CK*(BJ(L1)-BJ(L2))
      DO 3 I=1,M
      TX=Y(I)
      T=B*TX
      CALL BES(N2,T)
      K=I+MM
      CFP(K)=2*CJ*(TX*BJ(2)+BS*(BJ(1)-BJ(3)))
      CFT(K)=0.
      K=K+MD
      CFP(K)=-TX*(BJ(3)-BJ(1))-BS*(3*BJ(2)-BJ(4))
      CFT(K)=-CJ*(TX*(BJ(3)+BJ(1))-BS*(BJ(4)+BJ(2)))
      CK=CJ
      L1=3
      L2=1
      L3=4
      L4=2
```

```
      L5=0
      DO 3 J=3,N1
      CK=CK*CJ
      L1=L1+1
      L2=L2+1
      L3=L3+1
      L4=L4+1
      L5=L5+1
      K=K+MD
      CFP(K)=CK*CJ*(TX*(BJ(L1)-BJ(L2))+BS*(2*BJ(L4)-BJ(L3)-BJ(L5)))
3     CFT(K)=-CK*(TX*(BJ(L1)+BJ(L2))-BS*(BJ(L3)-BJ(L5)))
      K=0
      DO 7 I=1,ICASE
      FPE=0.
      FPH=0.
      FTE=0.
      FTH=0.
      FPEC=0.
      FPHC=0.
      FTEC=0.
      FTHC=0.
      TR=0.
      NS=IMS(I)+1
      NF=IMF(I)+1
      PH1=PHE(I)*PI/180.
      PH2=PHH(I)*PI/180.
      L=MD*(NS-1)
      DO 6 II=NS,NF
      SPQ=0.
      SPW=0.
      STW=0.
      STQ=0.
      J=II-1
      SN=(-1.)**J
      S1=SIN(J*PH1)
      C1=COS(J*PH1)
      S2=SIN(J*PH2)
      C2=COS(J*PH2)
      EN=1.
      FN=1.
      IF(J.NE.0)GO TO 4
      EN=.5
      FN=0.
4     DO 5 JJ=1,MD
      L=L+1
      K=K+1
      TERM=EN*(C1*Q(K)+CJ*S1*W(K))*CFP(L)
      FPE=FPE+TERM
      FPEC=FPEC+SN*TERM
      TERM=EN*(C2*Q(K)+CJ*S2*W(K))*CFP(L)
      FPH=FPH+TERM
      FPHC=FPHC+SN*TERM
      TERM=EN*(C1*W(K)+CJ*S1*Q(K))*CFT(L)
      FTE=FTE+TERM
      FTEC=FTEC+SN*TERM
```

```
      TERM=EN*(C2*W(K)+CJ*S2*Q(K))*CFT(L)
      FTH=FTH+TERM
      FTHC=FTHC+SN*TERM
      SPQ=SPQ+Q(K)*CFP(L)
      SPW=SPW+W(K)*CFP(L)
      STW=STW+W(K)*CFT(L)
5     STQ=STQ+Q(K)*CFT(L)
      SPN=EN*CABS(SPQ)**2+FN*CABS(SPW)**2
      STN=EN*CABS(STW)**2+FN*CABS(STQ)**2
6     TR=TR+SPN+STN*BC**2
      FTE=BC*FTE
      FTH=FTH*BC
      FTEC=FTEC*BC
      FTHC=FTHC*BC
      PATE=CABS(FTE)**2+CABS(FPE)**2
      PATEC=CABS(FTEC)**2+CABS(FPEC)**2
      PATH=CABS(FTH)**2+CABS(FPH)**2
      PATHC=CABS(FTHC)**2+CABS(FPHC)**2
      PE(I)=PATE*2/AREA
      PEC(I)=PATEC*2/AREA
      PH(I)=PATH*2/AREA
      PHC(I)=PATHC*2/AREA
7     TC(I)=TR*SIN(THETA)/AREA
      RETURN
      END
```

B-2.2. Main Program 2.

This program computes the power gain pattern and transmission coefficients for an aperture. A number of incidences are considered at the same time. Punch data cards are read according to the following input sequence:

```
101  FORMAT (I3)
102  FORMAT (10F6.1)
103  FORMAT (2E14.7, I3)
104  FORMAT (2I3)
105  FORMAT (5E14.7)
     READ (1,101) IT
     READ (1,101) ICASE
     READ (1,102) (PHE(I), I=1, ICASE)
     READ (1,102) (PHH(I), I=1, ICASE)
     READ (1,103) RO, RI, M
       MD = 2*M-1
        K = 1
        L = MD
       DO   2 I=1, ICASE
     READ (1,104) IMS(I), IMF(I)
     NSF = IMF(I) - IMS(I) + 1
       DO  2 J=1, NSF
     READ (1,105) (W(II), II=K,L)
     READ (1,105) (Q(II), II=K,L)
        K = K + MD
  2     L = L + MD
```

The input data is defined by

IT = number of points used in the range of θ from 0 to $\frac{\pi}{2}$ where pattern is computed.

ICASE = number of incidences considered.

PHE(i) = azimuthal angle (in degrees) specifying the first plane where pattern is computed for the ith incidence.

PHH(i) = azimuthal angle (in degrees) specifying the second plane where pattern is computed for the ith incidence.

RI, RO are the inner and outer radius (in wavelengths) of the aperture.

M = number of subdomains used.

IMS(i) = order of the lowest mode used for the ith incidence.

IMF(i) = order of the highest mode used for the ith incidence.

W store the $e_2 \bar{v}^{n\perp}$'s starting from the lowest mode of the first incidence

Q store the $e_1 \bar{v}^{n/\!/}$'s starting from the lowest mode of the first incidence

Minimum allocations are given by

```
COMPLEX    W(NW), Q(NW)
DIMENSION  PE(ICASE), PH(ICASE), PEC(ICASE), PHC(ICASE),
           TC(ICASE), PTE(NP), PTH(NP), TRAN(ICASE)
COMMON     /BLKF1/X(M-1), Y(M), IMS(ICASE), IMF(ICASE),
                  PHE(ICASE), PHH(ICASE)
```

where

$$NW = \sum_{i=1}^{ICASE} (2M-1)\ (IMF(i) - IMS(i) + 1)$$

$$NP = 2IT \cdot ICASE$$

The range 0 to $\frac{\pi}{2}$ of θ is divided into IT equal intervals. Power gain is computed at the centers of these intervals and the integration of (B-3) is done numerically using simple midpoint rules. DO loop 6 computes and store in PTE, PTH $G'(\theta,\phi)$ for 2IT θ's and both planes and all incidences. The first element of PTE is $G'(90° (1 - \frac{1}{IT}), PHE(1))$ and similarly for PTH. Transmission coefficients are also computed in DO loop 6. TRAN stores transmission coefficients for all incidences. $G(\theta,\phi)$ is computed according to (B-4) in DO loop 8 using $G'(\theta,\phi)$ and the transmission coefficient.

LISTING OF PROGRAM 2

```
      COMMON /BLKF1/X(50),Y(50),IMS(20),IMF(20),PHE(20),PHH(20)/BLKF2/W,
     6Q/BLKF3/ICASE,NMAX,M,AK,RI
      COMPLEX W(2000),Q(2000)
      DIMENSION PE(20),PH(20),TC(20),TRAN(20),PEC(20),PHC(20),PTE(3600),
     6PTH(3600)
101   FORMAT(I3)
102   FORMAT(10F6.1)
103   FORMAT(2E14.7,I3)
104   FORMAT(2I3)
105   FORMAT(5E14.7)
106   FORMAT('1',1X,'FIELD PATTERN',//)
107   FORMAT('1',1X,'CASE',I3,///,7X,'FIRST PLANE',3X,'SECOND PLANE',/,
     67X,'(',F5.1,'DEG.)',3X,'(',F5.1,'DEG.)',/)
108   FORMAT(1X,I3,2E14.4)
109   FORMAT(//,1X,'TRANSMISSION COEFFICIENT=',E11.4)
      READ(1,101)IT
      READ(1,101)ICASE
      READ(1,102)(PHE(I),I=1,ICASE)
      READ(1,102)(PHH(I),I=1,ICASE)
      READ(1,103)RO,RI,M
      PI=3.141593
      AK=2*PI*(RO-RI)/M
      IT2=IT*2
      MM=M-1
      MD=M+MM
      D=RO-RI
      X0=M*RI/D
      NMAX=0
      K=1
      L=MD
      DO 2 I=1,ICASE
      READ(1,104)IMS(I),IMF(I)
      NSF=IMF(I)-IMS(I)+1
      IF(IMF(I).LE.NMAX)GO TO 1
      NMAX=IMF(I)
1     DO 2 J=1,NSF
      READ(1,105)(W(II),II=K,L)
      READ(1,105)(Q(II),II=K,L)
      K=K+MD
2     L=L+MD
      T=X0
      DO 3 I=1,MM
      T=T+1.
3     X(I)=T
      T=X0-.5
      DO 4 I=1,M
      T=T+1.
4     Y(I)=T
      DT=PI/(2*IT)
      THETA=(PI+DT)/2.
      DO 5 I=1,ICASE
5     TRAN(I)=0.
```

```
      DO 6 I=1,IT
      THETA=THETA-DT
      CALL FAR(THETA,PE,PH,PEC,PHC,TC)
      K=I
      L=IT2+1-I
      DO 6 J=1,ICASE
      PTE(K)=PE(J)
      PTH(K)=PH(J)
      PTE(L)=PEC(J)
      PTH(L)=PHC(J)
      K=K+IT2
      L=L+IT2
6     TRAN(J)=TRAN(J)+DT*TC(J)
      K=0
      DO 7 I=1,ICASE
      DO 7 J=1,IT2
      K=K+1
      PTE(K)=PTE(K)/TRAN(I)
7     PTH(K)=PTH(K)/TRAN(I)
      WRITE(3,106)
      K=0
      LL=1-IT2
      DO 11 I=1,ICASE
      WRITE(3,107)I,PHE(I),PHH(I)
      DO 10 J=1,IT2
      K=K+1
      LL=LL+1
10    WRITE(3,108)J,PTE(K),PTH(K)
11    WRITE(3,109)TRAN(I)
      STOP
      END
```

SAMPLE OUTPUT

CASE 1

	FIRST PLANE (0.0DEG.)	SECOND PLANE (90.0DEG.)			
1	0.2195E 01	0.8660E-01	11	0.2181E 01	0.1306E 00
2	0.2195E 01	0.8741E-01	12	0.2178E 01	0.1393E 00
3	0.2194E 01	0.8903E-01	13	0.2175E 01	0.1487E 00
4	0.2193E 01	0.9145E-01	14	0.2171E 01	0.1589E 00
5	0.2192E 01	0.9468E-01	15	0.2168E 01	0.1697E 00
6	0.2191E 01	0.9870E-01	16	0.2164E 01	0.1813E 00
7	0.2189E 01	0.1035E 00	17	0.2160E 01	0.1936E 00
8	0.2188E 01	0.1091E 00	18	0.2156E 01	0.2066E 00
9	0.2186E 01	0.1155E 00	19	0.2151E 01	0.2202E 00
10	0.2183E 01	0.1227E 00	20	0.2146E 01	0.2345E 00

21	0.2141E 01	0.2494E 00	76	0.1598E 01	0.1334E 01
22	0.2136E 01	0.2649E 00	77	0.1586E 01	0.1345E 01
23	0.2131E 01	0.2810E 00	78	0.1573E 01	0.1355E 01
24	0.2125E 01	0.2977E 00	79	0.1561E 01	0.1365E 01
25	0.2119E 01	0.3149E 00	80	0.1548E 01	0.1374E 01
26	0.2113E 01	0.3327E 00	81	0.1536E 01	0.1382E 01
27	0.2106E 01	0.3509E 00	82	0.1523E 01	0.1389E 01
28	0.2100E 01	0.3697E 00	83	0.1511E 01	0.1395E 01
29	0.2093E 01	0.3889E 00	84	0.1498E 01	0.1401E 01
30	0.2086E 01	0.4086E 00	85	0.1486E 01	0.1406E 01
31	0.2079E 01	0.4287E 00	86	0.1473E 01	0.1410E 01
32	0.2071E 01	0.4492E 00	87	0.1461E 01	0.1413E 01
33	0.2064E 01	0.4701E 00	88	0.1449E 01	0.1415E 01
34	0.2056E 01	0.4913E 00	89	0.1436E 01	0.1417E 01
35	0.2048E 01	0.5128E 00	90	0.1424E 01	0.1418E 01
36	0.2039E 01	0.5346E 00	91	0.1412E 01	0.1418E 01
37	0.2031E 01	0.5567E 00	92	0.1400E 01	0.1417E 01
38	0.2022E 01	0.5790E 00	93	0.1388E 01	0.1415E 01
39	0.2014E 01	0.6015E 00	94	0.1375E 01	0.1413E 01
40	0.2005E 01	0.6242E 00	95	0.1363E 01	0.1410E 01
41	0.1995E 01	0.6471E 00	96	0.1351E 01	0.1406E 01
42	0.1986E 01	0.6701E 00	97	0.1340E 01	0.1401E 01
43	0.1977E 01	0.6932E 00	98	0.1328E 01	0.1395E 01
44	0.1967E 01	0.7164E 00	99	0.1316E 01	0.1389E 01
45	0.1957E 01	0.7396E 00	100	0.1304E 01	0.1382E 01
46	0.1947E 01	0.7628E 00	101	0.1293E 01	0.1374E 01
47	0.1937E 01	0.7861E 00	102	0.1281E 01	0.1365E 01
48	0.1927E 01	0.8093E 00	103	0.1270E 01	0.1355E 01
49	0.1916E 01	0.8324E 00	104	0.1259E 01	0.1345E 01
50	0.1906E 01	0.8554E 00	105	0.1247E 01	0.1334E 01
51	0.1895E 01	0.8783E 00	106	0.1236E 01	0.1323E 01
52	0.1884E 01	0.9010E 00	107	0.1225E 01	0.1310E 01
53	0.1873E 01	0.9236E 00	108	0.1214E 01	0.1297E 01
54	0.1862E 01	0.9459E 00	109	0.1203E 01	0.1284E 01
55	0.1851E 01	0.9681E 00	110	0.1193E 01	0.1269E 01
56	0.1840E 01	0.9899E 00	111	0.1182E 01	0.1254E 01
57	0.1829E 01	0.1011E 01	112	0.1172E 01	0.1239E 01
58	0.1817E 01	0.1033E 01	113	0.1161E 01	0.1222E 01
59	0.1805E 01	0.1054E 01	114	0.1151E 01	0.1206E 01
60	0.1794E 01	0.1074E 01	115	0.1141E 01	0.1188E 01
61	0.1782E 01	0.1094E 01	116	0.1131E 01	0.1171E 01
62	0.1770E 01	0.1114E 01	117	0.1121E 01	0.1152E 01
63	0.1758E 01	0.1133E 01	118	0.1111E 01	0.1133E 01
64	0.1746E 01	0.1152E 01	119	0.1101E 01	0.1114E 01
65	0.1734E 01	0.1171E 01	120	0.1092E 01	0.1094E 01
66	0.1722E 01	0.1188E 01	121	0.1083E 01	0.1074E 01
67	0.1710E 01	0.1206E 01	122	0.1073E 01	0.1054E 01
68	0.1698E 01	0.1222E 01	123	0.1064E 01	0.1033E 01
69	0.1685E 01	0.1239E 01	124	0.1055E 01	0.1011E 01
70	0.1673E 01	0.1254E 01	125	0.1046E 01	0.9899E 00
71	0.1661E 01	0.1269E 01	126	0.1038E 01	0.9681E 00
72	0.1648E 01	0.1284E 01	127	0.1029E 01	0.9459E 00
73	0.1636E 01	0.1297E 01	128	0.1021E 01	0.9236E 00
74	0.1623E 01	0.1310E 01	129	0.1012E 01	0.9010E 00
75	0.1611E 01	0.1323E 01	130	0.1004E 01	0.8783E 00

131	0.9963E 00	0.8554E 00	156	0.8469E 00	0.3149E 00
132	0.9885E 00	0.8324E 00	157	0.8430E 00	0.2977E 00
133	0.9808E 00	0.8093E 00	158	0.8392E 00	0.2810E 00
134	0.9733E 00	0.7861E 00	159	0.8356E 00	0.2649E 00
135	0.9659E 00	0.7628E 00	160	0.8322E 00	0.2494E 00
136	0.9587E 00	0.7396E 00	161	0.8290E 00	0.2345E 00
137	0.9516E 00	0.7164E 00	162	0.8259E 00	0.2202E 00
138	0.9447E 00	0.6932E 00	163	0.8229E 00	0.2066E 00
139	0.9379E 00	0.6701E 00	164	0.8201E 00	0.1936E 00
140	0.9313E 00	0.6471E 00	165	0.8175E 00	0.1813E 00
141	0.9248E 00	0.6242E 00	166	0.8151E 00	0.1697E 00
142	0.9185E 00	0.6015E 00	167	0.8128E 00	0.1589E 00
143	0.9124E 00	0.5790E 00	168	0.8107E 00	0.1487E 00
144	0.9064E 00	0.5567E 00	169	0.8087E 00	0.1393E 00
145	0.9005E 00	0.5346E 00	170	0.8069E 00	0.1306E 00
146	0.8949E 00	0.5128E 00	171	0.8053E 00	0.1227E 00
147	0.8893E 00	0.4913E 00	172	0.8038E 00	0.1155E 00
148	0.8840E 00	0.4701E 00	173	0.8025E 00	0.1091E 00
149	0.8788E 00	0.4492E 00	174	0.8014E 00	0.1035E 00
150	0.8737E 00	0.4287E 00	175	0.8004E 00	0.9870E-01
151	0.8689E 00	0.4086E 00	176	0.7996E 00	0.9467E-01
152	0.8641E 00	0.3889E 00	177	0.7989E 00	0.9145E-01
153	0.8596E 00	0.3697E 00	178	0.7984E 00	0.8903E-01
154	0.8552E 00	0.3509E 00	179	0.7981E 00	0.8741E-01
155	0.8510E 00	0.3327E 00	180	0.7979E 00	0.8660E-01

TRANSMISSION COEFFICIENT= 0.6142E-04

The magnetic current generated for case 2, $E_{//}$-polarization, in Section B-1.4 is used to generate the sample output above.

REFERENCES

[1] R. F. Harrington and J. R. Mautz, "A Generalized Network Formulation for Aperture Problems," Technical Report TR-75-13, November 1975, Syracuse University, Syracuse, New York, 13210.

[2] J. R. Mautz and R. F. Harrington, "Generalized Network Parameters for Bodies of Revolution, Technical Report TR-68-7, June 1968, Syracuse University, Syracuse, New York, 13210.

[3] R. F. Harrington, Time-Harmonic Electromagnetic Fields, McGraw-Hill Book Company, New York, 1969, Sec. 3-5.

[4] R. F. Harrington, Field Computation by Moment Methods, Macmillan Company, New York, 1968.

[5] A. W. Glisson and D. R. Wilton,"Simple and Efficient Numerical Techniques for Treating Bodies of Revolution," Phase Report RADC-TR-79-22, March 1979, University of Mississippi.

[6] H. A. Bethe, "Theory of Diffraction by Small Holes," Physical Review, second series, vol. 66, October 1944.

[7] B. D. Graves, T. T. Crow and C. D. Taylor, "On the Electromagnetic Field Penetration Through Apertures, IEEE Trans. on Electromagnetic Compatibility, vol. EMC-18, No. 4, November 1976.

[8] J. R. Mautz and R. F. Harrington,"Transmission from a Rectangular Waveguide into Half Space Through a Rectangular Aperture," Technical Report TR-76-5, May 1976, Syracuse University, Syracuse, New York 13210.

[9] M. Abramowitz and I. A. Stegun, Handbook of Mathematical Functions, U. S. Government Printing Office, Washington, D.C. (National Bureau of Standards, U.S. Applied Math. Ser. 55), 1964.